

1. Report No. SWUTC/08/473700-00088-1	2. Government Accession No.	3. Recipient's Catalog No.	
4. Title and Subtitle MEASURING THE MARGINAL COST OF CONGESTION		5. Report Date December 2008	6. Performing Organization Code
7. Author(s) Mark Burris and Sunil Patil		8. Performing Organization Report No. Report 473700-00088-1	
9. Performing Organization Name and Address Texas Transportation Institute Texas A&M University System College Station, Texas 77843-3135		10. Work Unit No. (TRAIS)	11. Contract or Grant No. DTRS99-G-0006
12. Sponsoring Agency Name and Address Southwest Region University Transportation Center Texas Transportation Institute Texas A&M University System College Station, Texas 77843-3135		13. Type of Report and Period Covered	14. Sponsoring Agency Code
15. Supplementary Notes Supported by a grant from the U.S. Department of Transportation, University Transportation Centers Program.			
16. Abstract <p>This study attempted to estimate the effect of additional vehicles joining the traffic stream when it is near capacity. The study used data from highways I-35, I-45 in Texas and I-80 in California aggregated at different time intervals. Various macroscopic traffic flow models, Catastrophe model and the bottleneck model were studied in order to identify models that best represent the speed-flow relation for the traffic data over complete range of flow.</p> <p>The Catastrophe model and the bottleneck model did not fit the data well, while three macroscopic models, the Modified HCM, Newell-Franklin and Van Aerde model were found to fit the data well. Using congestion pricing theory the optimum toll rates were calculated for each of these three models. The optimum toll rates were then compared with the toll rates on some of the existing variably priced toll roads the US. The optimum toll rates estimated using Modified HCM, Newell-Franklin and Van Aerde model were \$0.65, \$0.81 and \$0.97 per mile assuming the value of travel time savings as \$20/hr for the near capacity flow. These toll rates were found to be lower when compared with the maximum toll rates on three of the existing variable toll facilities which charge about \$1/mile during the hours of extreme congestion.</p>			
17. Key Words Marginal Cost of Congestion, Congestion Pricing, Traffic Flow Models, Catastrophe Theory		18. Distribution Statement No restrictions. This document is available to the public through NTIS: National Technical Information Service 5285 Port Royal Road Springfield, Virginia 22161	
19. Security Classif.(of this report) Unclassified	20. Security Classif.(of this page) Unclassified	21. No. of Pages 70	22. Price

Measuring the Marginal Cost of Congestion

by

Mark Burris

Associate Research Engineer

and

Sunil Patil

Graduate Assistant Research

Report SWUTC/08/473700-00088-1

Sponsored by the

Southwest Region University Transportation Center

December 2008

Texas Transportation Institute

Texas A&M University System

College Station, Texas

ACKNOWLEDGEMENT

The authors recognize and appreciate that support for this research was provided by a grant from the U.S. Department of Transportation, University Transportation Centers Program to the Southwest Region University Transportation Center.

DISCLAIMER

The contents of this report reflect the views of the authors, who are responsible for the facts and the accuracy of the information presented herein. This document is disseminated under the sponsorship of the Department of Transportation, University Transportation Centers Program, in the interest of information exchange. Mention of trade names or commercial products does not constitute endorsement or recommendation for use.

ABSTRACT

This study attempted to estimate the effect of additional vehicles joining the traffic stream when it is near capacity. The study used data from highways I-35, I-45 in Texas and I-80 in California aggregated at different time intervals. Various macroscopic traffic flow models, Catastrophe model and the bottleneck model were studied in order to identify models that best represent the speed-flow relation for the traffic data over complete range of flow.

The Catastrophe model and the bottleneck model did not fit the data well, while three macroscopic models, the Modified HCM, Newell-Franklin and Van Aerde model were found to fit the data well. Using congestion pricing theory the optimum toll rates were calculated for each of these three models. The optimum toll rates were then compared with the toll rates on some of the existing variably priced toll roads the US. The optimum toll rates estimated using Modified HCM, Newell-Franklin and Van Aerde model were \$0.65, \$0.81 and \$0.97 per mile assuming the value of travel time savings as \$20/hr for the near capacity flow. These toll rates were found to be lower when compared with the maximum toll rates on three of the existing variable toll facilities which charge about \$1/mile during the hours of extreme congestion.

EXECUTIVE SUMMARY

This study estimated the marginal cost of traffic congestion by quantifying the effects of additional vehicles entering the traffic flow. A brief literature review of macroscopic traffic flow models and congestion pricing theory was carried out to select speed-flow models which represent real world traffic data, especially near the congested conditions of traffic. Using these models and congestion pricing theory, the marginal cost of congestion was estimated and compared with the toll rates on the existing highway facilities in the US with variable toll rates. The study used three different data sets, loop detector data from I-35 in San Antonio, Wavetronix radar data from I-45 in Houston and video data from I-80 collected as part of NGSIM program in San Francisco bay area. I-35 and I-45 data were collected at 20 and 30 seconds intervals whereas the I-80 data was from individual vehicles. The vehicle trajectories from the NGSIM data were converted to the speed flow data which indicated that the data were only from hyper-congested part of speed flow relation. Hence, the NGSIM data set was not used since this study required data full spectrum of speed flow relationship.

Application of Catastrophe theory was investigated using I-35 and I-45 data sets. An alternative calibration technique using Genetic Algorithms was proposed. The Catastrophe model was found to predict speed only in two different speed groups and it did not represent the speed flow data well, hence was not used for further analysis.

Three macroscopic models, the Modified HCM, Newell-Franklin and Van Aerde model were found to fit the data well. Data collected on I-45 was analyzed to find the values such as capacity, free flow speed and the speed at capacity, used in these models. These models after calibration represented the speed flow data well. The performance of these models was then compared with the bottleneck model which did not fit the speed flow relationship well.

Using congestion pricing theory the marginal cost of congestion was estimated for Modified HCM, Newell-Franklin and Van Aerde models and it was found to be \$0.65, \$0.81 and \$0.97 per mile near capacity assuming the value of travel time savings as \$20/hr. When compared to the maximum toll rates on some of the existing facilities with variable pricing (SR-91 California- \$0.95/mile, SR-167 Washington- \$1/mile and I-15 San Diego- \$1/mile), the estimated toll rates were found to be slightly lower than those in use.

TABLE OF CONTENTS

1 INTRODUCTION	1
2 LITERATURE REVIEW	3
Traffic Flow Models	3
Single-regime Models.....	3
Multi-Regime Models.....	5
Vickery's Bottleneck Model.....	7
Congestion Pricing	8
3 DATA.....	11
I-35 Loop Detector Data.....	11
I-45 Wavetronix Radar Data.....	11
Vehicle Trajectory Data from I-80	12
4 DATA ANALYSIS.....	13
Variation of Capacity, Free-Flow Speed and Speed at Capacity	13
NGSIM data Analysis.....	15
5 APPLICATION OF THE CATASTROPHE THEORY	19
Data Transformation for Catastrophe Theory	21
Calibration of the Catastrophe Model	21
Genetic Algorithm Approach for Calibration of the Catastrophe Model	22
6 APPLICATION OF MACROSCOPIC TRAFFIC FLOW MODELS.....	29
Modified HCM Model.....	29
Re-specified Newell-Franklin Model	30
Van Aerde Model	31
Application of the Data.....	31
Comparison with Vickery's Bottleneck Model	32
7 APPLICATION OF CONGESTION PRICING THEORY.....	35
Calculation of Toll Rates.....	36
Sensitivity of Toll Estimation to the Value of Capacity.....	38
Comparison of the Optimum Toll Rates with Toll Rates on Existing Variable Priced Toll Lanes.....	39
8 CONCLUSIONS	41
REFERENCES	43

LIST OF FIGURES

FIGURE 1 Speed, Flow and Density Relationship Plots for Greenshield's Model	5
FIGURE 2 Qualitative presentation of Traffic Flow Regimes on the Background Speed-flow data in Ayalon Freeway, Tel-Aviv, Israel	6
FIGURE 3 Speed-Demand Curve for Vickery's Bottleneck Model	8
FIGURE 4 Marginal Cost Curve and Congestion Toll	9
FIGURE 5 Capacity, FFS and Speed at Capacity of the Section on Different Days	14
FIGURE 6 Variation in Maximum Hourly Volume and Maximum Flow rate	14
FIGURE 7 Variation in Speed at Capacity.....	15
FIGURE 8 Speed Flow Plot for NGSIM Data using 2 Second Time Aggregation	16
FIGURE 9 Speed Flow Plot for NGSIM Data using 5 Second Time Aggregation	16
FIGURE 10 Speed Flow Plot for NGSIM Data using 10 Second Time Aggregation	17
FIGURE 11 Speed Flow Plot for NGSIM Data using 20 Second Time Aggregation	17
FIGURE 12 General Shape of Cusp Catastrophe Surface and its Three Dimensional View Created using Matlab.....	19
FIGURE 13 Maxwell's Convention for the Catastrophe Surface	20
FIGURE 14 U2 (Volume) vs. V2 (Occupancy) following Axes Transformation.....	23
FIGURE 15 Volume vs. Occupancy data Following Graphical Transformation and Axes Rotation	23
FIGURE 16 Prediction Success for Catastrophe Theory using Hall's Approach	24
FIGURE 17 U2 (Volume) vs. V2 (Occupancy) following Axes Transformation using Trial and Error for Critical Values	25
FIGURE 18 Volume vs. Occupancy Data Following Graphical Transformation and Axes Rotation Using Trial and Error For Critical Values	25
FIGURE 19 Prediction Success for Catastrophe Theory using Trial and Error for Critical Values	26
FIGURE 20 Three Dimensional Plot for the Prediction Success of Catastrophe Theory	26
FIGURE 21 Prediction Success for Catastrophe Theory using I-45 Wavetronix Data.....	27
FIGURE 22 Optimum α Value for Modified HCM Model.....	30
FIGURE 24 Congestion Toll Estimation for Various Traffic Flow Models at Different Flow Levels.....	37
FIGURE 25 Congestion Toll Estimation for Near Capacity Flow Values for Various Traffic Flow Models	37
FIGURE 26 Effect of Capacity Value on the Toll Rate Estimation for Flow Equal to 99 percent of Capacity.....	39

LIST OF TABLES

TABLE 1 Characteristics of Various Single-Regime Models.....	4
TABLE 2 Equations and Breakpoints for Two-Regime Models	6
TABLE 3 Sensitivity of Toll Estimation for Assumed Capacity Values	38
TABLE 4 Comparison of Toll Rates on SR-91 and SR-167 with the Optimum Toll Rates.....	40

1 INTRODUCTION

Congestion pricing is gaining popularity in the United States and quantifying the effects of an additional vehicle joining the traffic stream is a critical issue to determine the toll rates and benefits from pricing. When additional vehicles enter a crowded roadway they increase travel time for all vehicles. The effect of additional vehicles worsens when the flow is near the capacity of the traffic stream. The speed and flow of the traffic stream are considered as the major variables to quantify these effects. Hence to better understand and quantify this issue it is necessary to accurately model the traffic stream near capacity. This study attempts to quantify the marginal cost of congestion by fitting a traffic flow model and then using that model to predict the congestion toll.

Chapter 2 of this report contains a brief literature review of the traffic flow models and theory of congestion pricing. Chapter 3 contains the description of the data used in this study. Chapter 4 contains analysis of the data in order to find the critical parameters needed for calibration of the traffic flow models; the capacity, free flow speed and the speed at capacity. It also contains a description of the data processing required for using the vehicle trajectory data for macroscopic traffic flow modeling.

Chapter 5 discusses the application of the catastrophe theory. Chapter 6 discusses calibration of the macroscopic traffic flow models and Chapter 7 contains the congestion pricing application to the selected traffic flow models and estimating the marginal cost of congestion. Also, in this chapter, the toll rates observed on some of the existing facilities are compared with the optimum toll rates estimated in this study.

2 LITERATURE REVIEW

In order to quantify the effect of additional vehicles joining the traffic stream, it is necessary to model the characteristics of traffic flow. Speed, flow and density are considered to be the fundamental characteristics of the traffic stream, out of which speed and flow have been traditionally used to define the state of traffic. This study begins by reviewing various traffic flow models for their applicability and accuracy. The theory of congestion pricing is also reviewed to estimate the monetary cost of the effects of additional vehicles joining the traffic stream.

Traffic Flow Models

Traffic flow models provide the fundamental relationships of macroscopic traffic flow characteristics for uninterrupted flow situations. Traffic flow models are used in the planning, design, and operations of transportation facilities.

Over the years, a number of traffic flow models have been proposed. Some of them are based on analogies to other fields, e.g. Greenberg used hydrodynamic analogy in which he assumed traffic flow analogues to a continuous fluid (Greenberg 1959). The earlier models assumed a single regime phenomenon over the complete range of flow conditions, including free-flow and congested flow situations. Later models attempted to improve on the earlier models by considering separate regimes (e.g. a free-flow regime and a congested-flow regime) and attempted to generalize by introducing additional parameters that could be used to distinguish between roadway environments (May 1990).

Single-regime Models

Some of the frequently used single-regime models and their characteristics are shown in Table 1. Typical plots for speed , flow and density using the Greenshield model are shown in Figure 1.

TABLE 1 Characteristics of Various Single-Regime Models

Single-regime models	Limitations
Greenshield Model $q = K_j V \left(1 - \frac{V}{V_f} \right)^{1/\beta}$	Underestimation of jam density
Greenberg Model $q = k_j V \exp\left(-\frac{V}{V_o}\right)$	Underestimation of maximum flow Overestimation of free flow speed (infinity) Underestimation of optimum speed
Underwood Model $q = k_o V \left(\delta \ln\left(\frac{V_f}{V}\right) \right)^{\frac{1}{\delta}}$	Underestimation of maximum flow Overestimation of free flow speed Overestimation of jam density (infinity)
(Simplified) HCM 2000 Model (Li 2008,HCM 2000) $q = q_o \left[\frac{V_f - V}{V_f - V_o} \right]^{\frac{1}{\beta}}, \beta \geq 1$	Only applicable for $V_o \leq V \leq V_f$ or not applicable for the hyper-congested part of speed flow curve

Source: (May 1990)

Notations used in Table 1 are as follows:

V = Space mean speed,

k = Density,

q = flow,

V_f = Free-flow speed,

k_j = Jam density,

V_o = Optimum speed,

k_o = Optimum density,

q_o = Maximum Flow (Capacity)

Apart from these models Drew and Pipes-Munjal proposed generalized single-regime models with additional parameter ‘n’. The value of ‘n’ changes the nature of the speed-density relationship from linear to exponential and thus a spectrum of traffic stream models can be formulated. The most serious drawback of single regime models is their inability to represent the measured field data near capacity conditions (May 1990). Aerde and Rakha (1995) developed an auto calibration technique for multivariate calibration of single regime speed-flow-density relationships (Van Aerde and Rakha 1995). This procedure provided a fit that was found reasonable for all data regimes. This model has been described in detail in Chapter 7. Li (2008) proposed additional parameter models as described in the Chapter 7 of this report. Li added some parameters to the popular models in order to add some flexibility by introducing the concept of

speed-elasticity of the flow and using a set of primitive conditions that are associated with monotonicity property of the speed-density curve and the backward-bending property of speed-flow curve. He also proposed some changes to the HCM 2000 model to extend it for the (hyper) congested region by adding one more parameter (Li 2008).

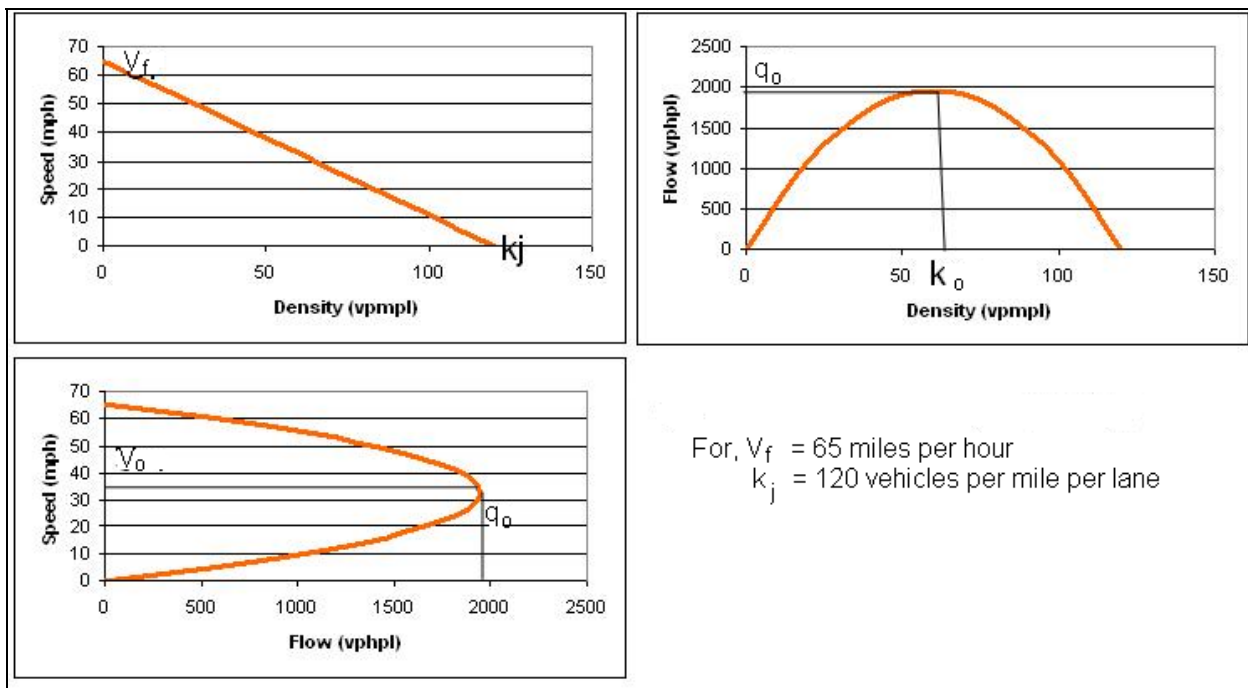


FIGURE 1 Speed, Flow and Density Relationship Plots for Greenshield's Model

Multi-Regime Models

Multi-regime models use different speed density relationships for different flow conditions to overcome some of the limitations of the single-regime models. Three main regimes of the speed density relationship are shown in Figure 2.

Some popular two-regime models are listed in Table 2. One of difficulties faced by the two-regime models is determining the breaking point between regimes. The estimates of the breaking points given by Northwestern university research team are shown in Table 2 (May 1990). When compared with actual freeway data it was found that overall two-regime models perform better than any of the older single-regime models listed above (Greenshield, Greenberg and Underwood model) in tracking the freeway data set.

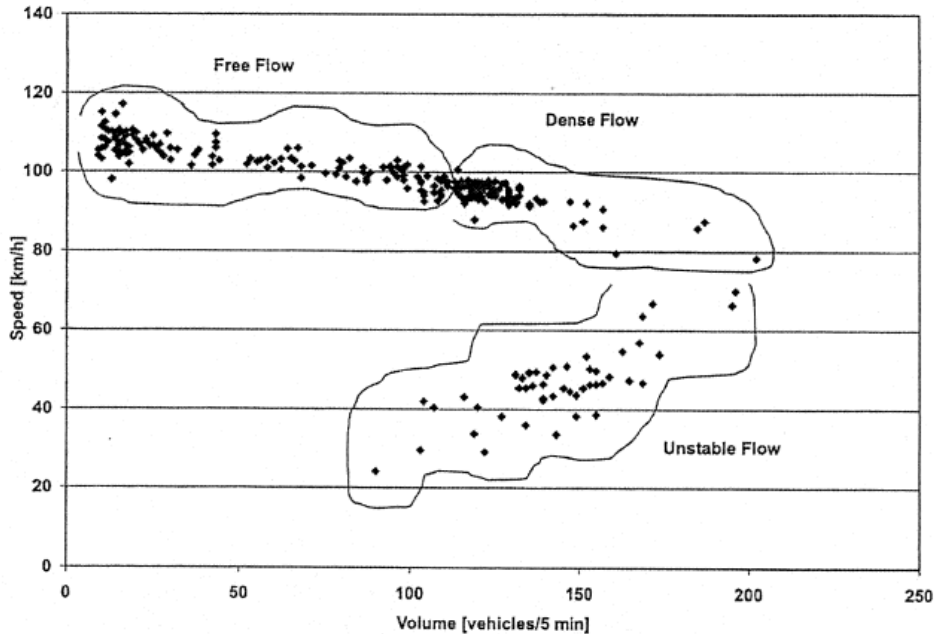


FIGURE 2 Qualitative presentation of Traffic Flow Regimes on the Background Speed-flow data in Ayalon Freeway, Tel-Aviv, Israel (Polus and Pollatschek 2002, Bassan 2005)

TABLE 2 Equations and Breakpoints for Two-Regime Models

Two-Regime Model	Free-Flow Regime	Congested-Flow Regime
Modified Greenberg Model	Constant speed 48 ($k \leq 35$)	Greenberg model $U = 32 \ln\left(\frac{145.5}{k}\right)$ ($k \geq 35$)
Two-regime Linear Model	Greenshield Model $U = 60.9 - 0.515k$ ($k \leq 65$)	Greenshield Model $U = 40 - 0.265k$ ($k \geq 65$)
Edie Model	Underwood Model $U = 54.9 e^{\frac{-k}{163.9}}$ ($k \leq 50$)	Greenberg model $U = 26.8 \ln\left(\frac{162.5}{k}\right)$ ($k \geq 50$)

Two-regime models have smaller mean deviations than those of the single-regime models. As per May (1990), the Edie model slightly overestimates the maximum flow while the other two slightly underestimate the maximum flow. The linear two-regime model slightly overestimates free-flow speed and the modified Greenberg model slightly underestimates free-flow speed. The optimum speed is slightly overestimated by the Edie model. All models underestimate jam density significantly. Although the two-regime models provide a considerable

improvement over single-regime models, their component models appear discretely different (May 1990).

The three-regime model considers free-flow regime, transitional flow regime, and congested-flow regime, each being represented by the Greenshield's formulation. Three-regime models also face the difficulty in determining the breakpoint between regimes. Overall multi-regime models represent field data well and much better than many initial single-regime models (May 1990). However this study needs a model which is continuous in nature and which can be easily adapted into the congestion pricing theory. A single-regime model that fits the available freeway data collected at smaller time intervals is needed for this study.

Numerous theories and models have been proposed for modeling the speed flow relationship. The literature clearly shows that there are many problems in modeling the traffic flow and there are many issues that need to be considered, as given below:

- Downstream conditions (such as construction) can affect the speed-flow curve (Zhou and Hall 1999),
- Different freeways have different parameters hence different equations (Zhous and Hall 1999),
- Traffic flow can not be assumed to be uniform in congested flow conditions (Banks 1999),
- Flow phases, flow-concentration relationships and transitions to congested flow is very diverse (Banks 2002),

Vickery's Bottleneck Model

Vickery's bottleneck model is a microscopic traffic flow model which has been used in the congestion pricing literature (Vickery 1969). The speed-flow curve for the Vickery's bottleneck model can be developed by using simple logic. The bottleneck model calculates the travel time based on a queue that forms once demand exceeds capacity.

The length of the queue is given by the difference between the departure rate $r(t)$ at time t and the capacity, when the departure rate is more than the capacity (q_o).

$$\text{Queue length, } Q(t) = r(t) - q_o;$$

Hence the waiting time in queue, $T^w(t) = Q(t) / q_o$ and the total travel time

$$T(t) = \bar{T} + T^w(t);$$

where \bar{T} =fixed component travel (which can be calculated as 1/free flow speed for one mile long segment)

Hence, the speed for the one mile long segment (only when the departure rate is more than the capacity) can be calculated as

$$\text{Speed } (t) = 1/T(t) = \frac{1}{\bar{T} + \frac{Q(t)}{q_o}} = \frac{1}{\frac{1}{V_f} + \frac{r(t)-q_o}{q_o}} = \frac{q_o \times V_f}{q_o + V_f(Demand - q_o)};$$

Further the bottleneck model assumes that the flow is equal to demand when it is less than the capacity of the bottleneck and it is equal to capacity when the demand exceeds the capacity. This results in a constant speed (equal to the free flow speed) for all the flow values below capacity. The resulting speed-demand curve for Vickery's Bottleneck model (for a free flow speed of 64 miles per hour and bottleneck capacity as estimated in the chapter 4 to be 1684 vehicles per hour) is shown in Figure 3.

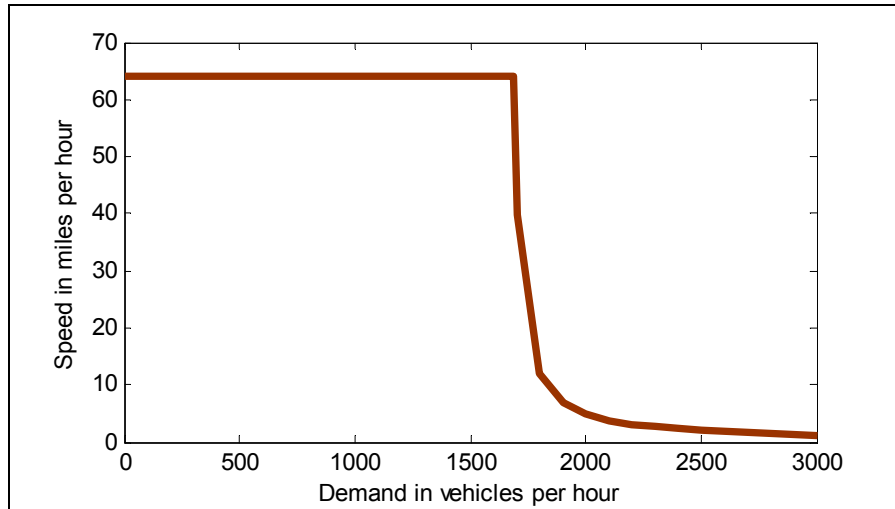


FIGURE 3 Speed-Demand Curve for Vickery's Bottleneck Model

Congestion Pricing

Walters (1961) illustrated the use of a speed-flow curve in applying the theory of congestion pricing. Simple economic principles can be applied in derivation of the tolls for pricing. The Average Variable Cost (AVC) curve is obtained by multiplying the travel time-flow curve by the average generalized cost (including time cost). The upward bending slope of

the AVC is mainly due to the time cost since it can be safely assumed that the operating costs of a vehicle change little with traffic flow when compared to time costs. As shown in Figure 4 the AVC curve takes the backward bending shape due to similar backward bending nature of the speed flow curve (see Figure 1).

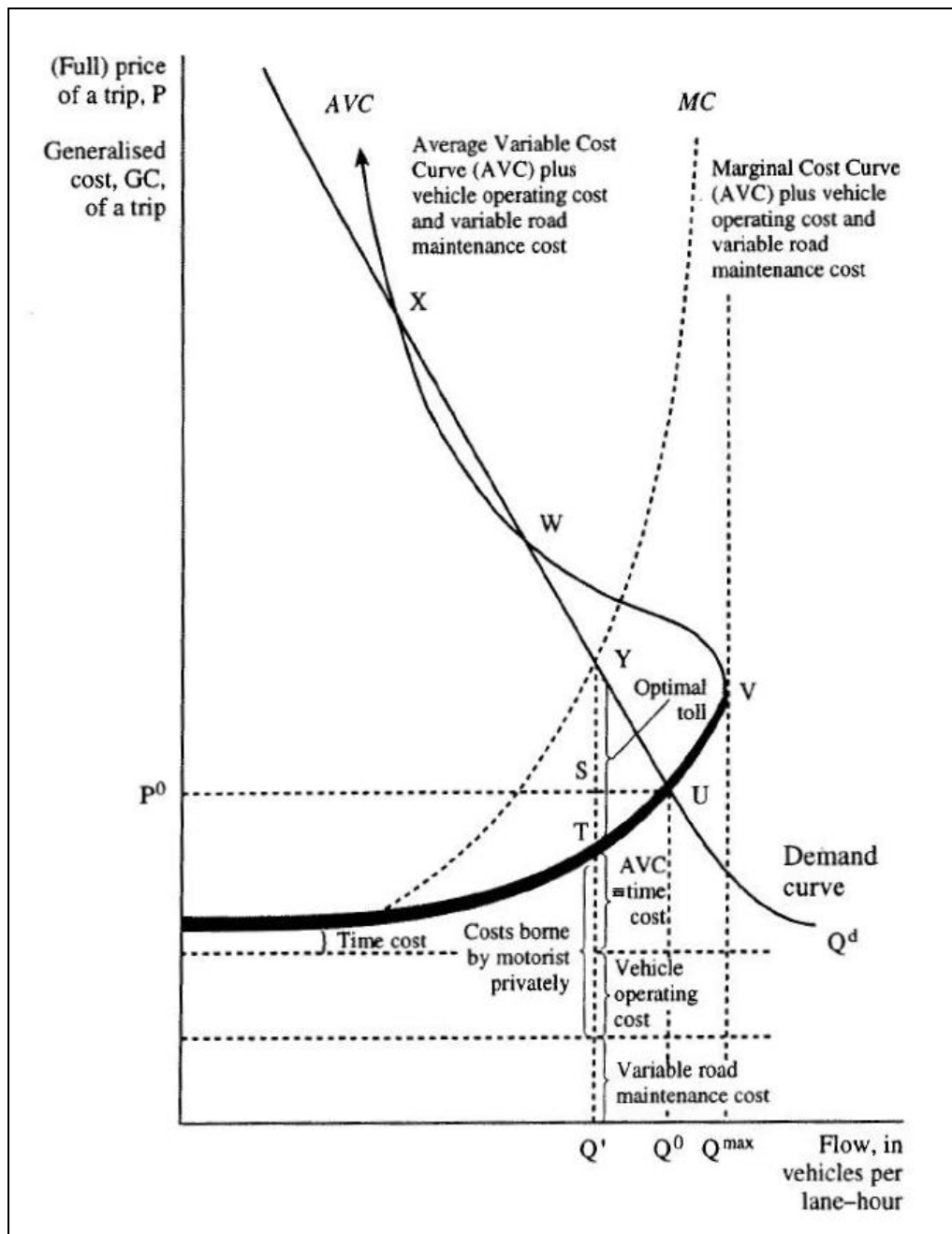


FIGURE 4 Marginal Cost Curve and Congestion Toll (Source: Button and Verhoeff 1998)

The additional delay (cost) that one driver imposes on the rest of the drivers is the difference between the marginal cost (MC) curve and the AVC curve. Hence the optimum toll should be equal to the difference between the MC curve and the AVC to make the most efficient use of the facility (road).

3 DATA

In order to quantify the effects of vehicles entering the traffic stream near the congestion point, this study needed traffic flow data collected at short time intervals. Accurate values of speed and flow are crucial in the calibration of any traffic flow model. With the advancement of technology various new data collection techniques are available. One of the interesting features of this study is that it used traffic data from various sources at various locations gathered at different time intervals using different technologies/instruments. Most of the data comes from I-35 in San Antonio (loop detector data collected at 20 seconds interval) and Wavetronix radar data (collected at 30 seconds interval) from I-45 North in Houston. We have also used data from NGSIM (Next Generation Simulation) program which has vehicle trajectory data on eastbound I-80 in the San Francisco Bay area collected using video cameras.

I-35 Loop Detector Data

Speed and volume data collected from loop detectors located on I-35 northeast of San Antonio every 20 seconds was used in this study (Carter and Burgess 2002). This study uses data from only one location. The data used for this study was collected at the mile marker location 159.5 (at New Braunfels Avenue) on I-35 south bound in northeast part of San Antonio which has 3 lanes in each direction. This location is not near to any of the freeway ramps.

In order to remove the erroneous data various filtering criteria were used. Data entries with zero speed at non-zero volume or a volume of more than 18 vehicles (in 20 seconds) were discarded. Also, since the data was collected at every 20 seconds it was decided to use the data only from 3/10/2003 to 3/14/2003 collected from time “15:29:44” onwards till “20:30:33” each day (which resulted in about 4500 data points) to capture the full spectrum of the speed flow curve but still have a data set that was small enough to work with.

I-45 Wavetronix Radar Data

Radar data collected using Wavetronix equipment at 30 second intervals were made available for this study. The data was collected for 45 days, during the time period between January to August 2006. The data used were from the section of I-45 North at Airline Street away from any of the freeway ramps. That section of I-45 has four lanes in each direction. The average data across all the lanes in northbound direction was used for calculating the speed and

volume per lane. Whenever the data from one or more lanes out of the total four lanes was missing the average volume was adjusted accordingly. This resulted in 1440 data points corresponding to each day. Further, the data entries corresponding to zero speed at a non-zero volume and volume more than 26 vehicles (in 30 seconds) were discarded.

Vehicle Trajectory Data from I-80

As a part of the NGSIM program, detailed vehicle trajectory data on eastbound I-80 in the San Francisco Bay area in Emeryville, CA, was collected on April 13, 2005 (NGSIM 2008). This vehicle trajectory data is available for download (at <http://ngsim.fhwa.dot.gov/>). The data has been extracted from synchronized digital cameras and is believed to be one of the best microscopic data sets available. These data provide the precise location of each vehicle within the study area every one-tenth of a second, resulting in detailed lane positions and locations relative to other vehicles. A total of 45 minutes of data are available in the full dataset. It is segmented into three 15-minute periods: 4:00 p.m. to 4:15 p.m.; 5:00 p.m. to 5:15 p.m.; and 5:15 p.m. to 5:30 p.m. which represent the transition from near capacity condition to hyper congested condition. Unfortunately the uncongested data and the data corresponding to the region of free flow to moderate congestion were not available in the trajectory format and it was beyond the scope of this study to convert the video data into trajectory data.

4 DATA ANALYSIS

It was necessary to estimate the values of critical parameters such as capacity and free flow speed in order to calibrate the macroscopic traffic flow models. The value of capacity varies based on several factors such as geometry of the section of highway, type of vehicles etc. Hence it is necessary to study this variation in order to use an average value for calibration. This section of the study uses the I-45 data set collected at a section of the freeway which has four lanes and is away from any ramps.

This section also describes the methodology of converting the vehicle trajectory data into speed flow data.

Variation of Capacity, Free-Flow Speed and Speed at Capacity

The capacity of a roadway plays an important role in fitting a traffic flow model to the data. The capacity as defined in HCM 2000 is the “maximum hourly rate of vehicles or persons that can reasonably be expected to pass a point, or traverse a uniform section of lane or roadway, during a specified time period under prevailing conditions (traffic and roadway)”(HCM 2000). The capacity is not constant for a roadway, it varies according to different factors such as geometry, day of week, weather, etc. Hence, the capacity analysis explained below was carried out for data collected on 45 days to capture the variation in capacity.

The definition of Free Flow Speed (FFS) used for this study is the average speed that a vehicle would travel if there were no congestion (flow is less than 600 vehicles per hour) or other adverse conditions.

The Wavetronix data set from I-45 had data corresponding to different days at different locations. Data corresponding to 45 days was extracted for the study location (I-45 at Airline street). After filtering the data and averaging it for all lanes in a direction the capacity, free flow speed and (optimum) speed at capacity were extracted from each day’s data. The variation in capacity for all the 45 days is shown in Figure 5.

The average values for these variables were as follows:

- Capacity- 2472 veh/hr (flow rate from 30 sec data), 1684 veh/hr (hourly volume)
- Free flow speed- 64 mph
- Optimum speed- 54 mph

Instead of estimating hourly flows using the 30 second counts, it was also possible to obtain the hourly volume at any time interval by simply counting the cars during the hour long period. The hourly volume and flow rate are shown in Figure 6 with the corresponding speeds at capacity shown in Figure 7.

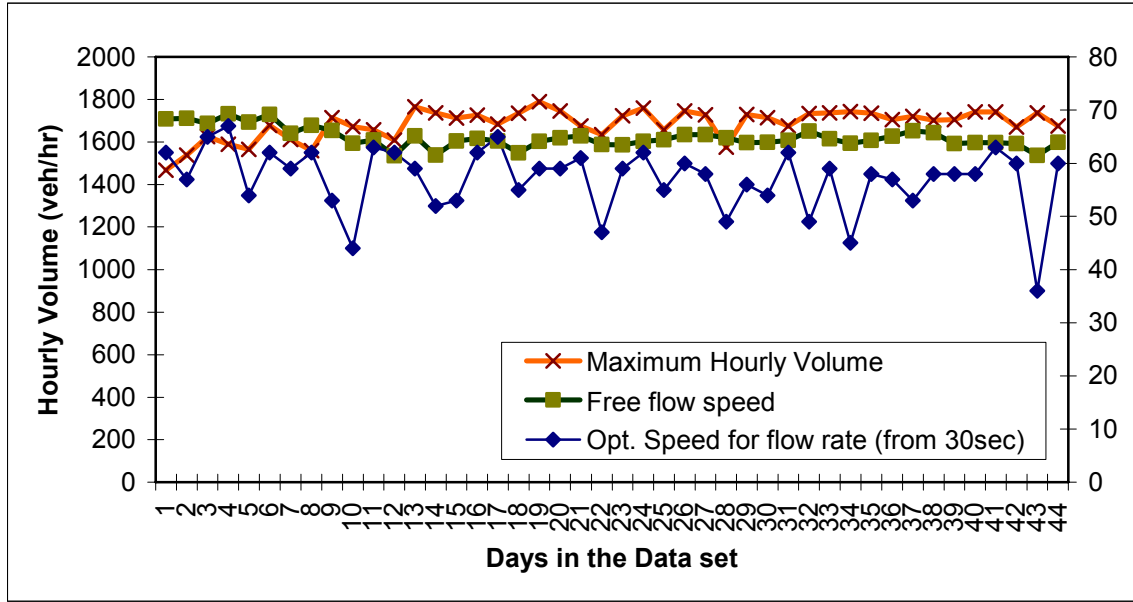


FIGURE 5 Capacity, FFS and Speed at Capacity of the Section on Different Days

As expected, the hourly volume is considerably smaller than the hourly flow rate obtained using 30 second counts.

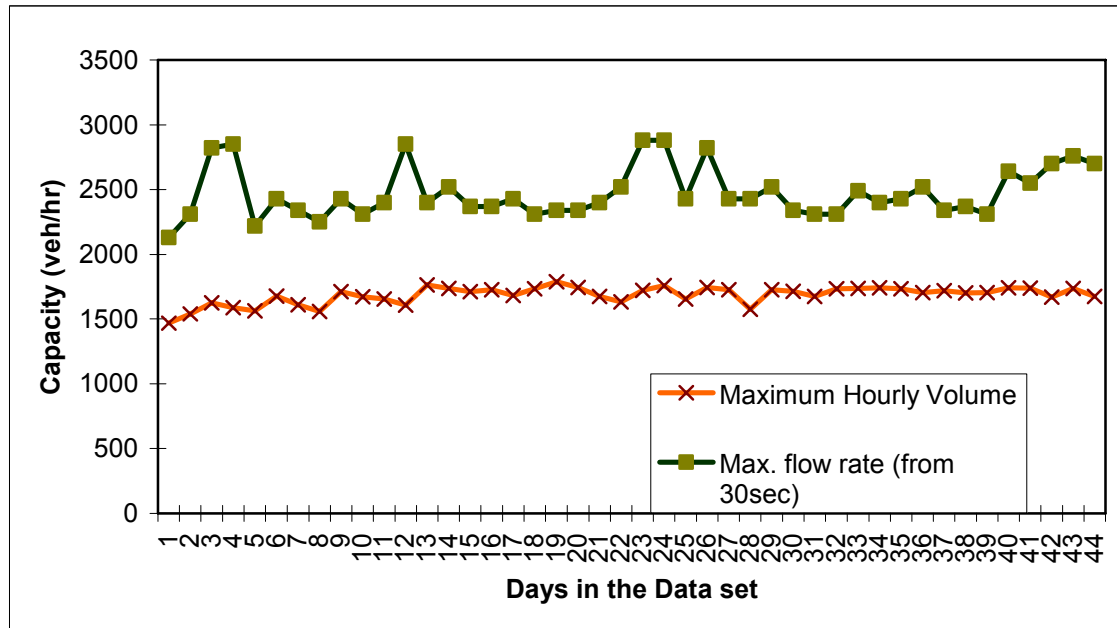


FIGURE 6 Variation in Maximum Hourly Volume and Maximum Flow rate

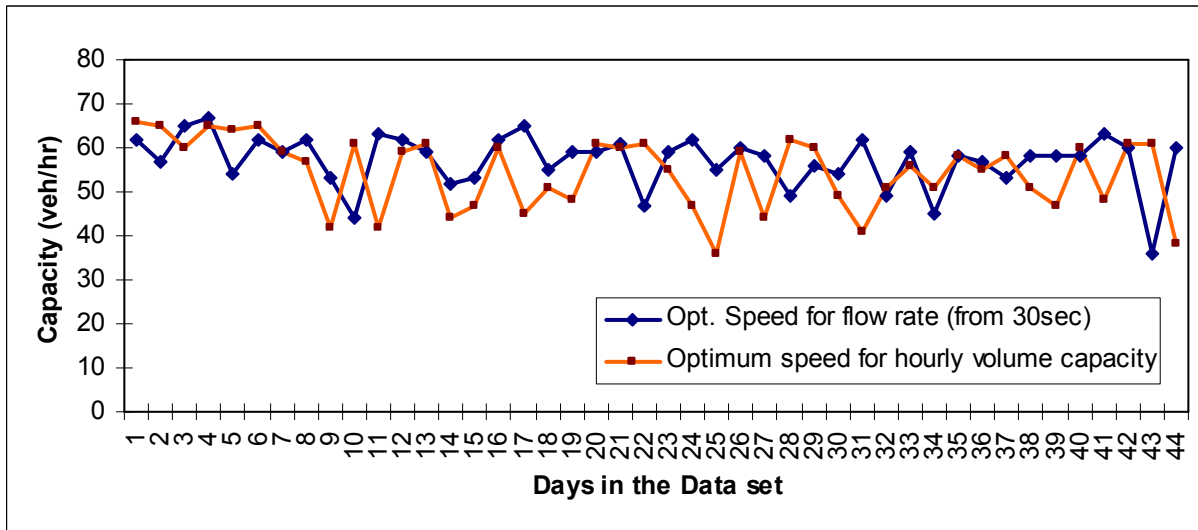


FIGURE 7 Variation in Speed at Capacity

NGSIM data Analysis

NGSIM data was in the form of vehicle trajectories. The position of each vehicle was given for every one-tenth of a second. In order to use this data for fitting a macroscopic traffic model it was necessary to convert the individual trajectory data into speed-flow data for the stream. By calculating the time required for a vehicle to travel a 200 feet section of the freeway its speed was estimated. Further using a time aggregation value (such as 20 seconds) one can find the flow and density from the given trajectories. Unlike other data sets where it is not possible to physically measure the density, this data set offers an option of doing so. For any given time the number of vehicles in the given section, and hence the density, can be observed. The Matlab (Math Works 1994) code given in Appendix A-1 was used to determine the speed, flow and density for this data set. It is possible to change the section length, and time aggregation in this code. Figure 8 through Figure 11 depict the speed flow plots for various time aggregations. The flow values were calculated in two different ways as shown in these figures. It can be observed that all the data lies in the congested and hyper-congested part of the speed-flow curve. It was necessary to have the free-flow and uncongested condition data along with the data near capacity in order to use it for calibration of the traffic flow models and study the near breakdown conditions, hence this data set was not used further. Instead the data sets from I-35 and I-45 as described in Chapter 3 were used for further analysis. These data sets provided the whole range of speed flow data points collected on different days at intervals of 20 (I-35) and 30 (I-45) seconds.

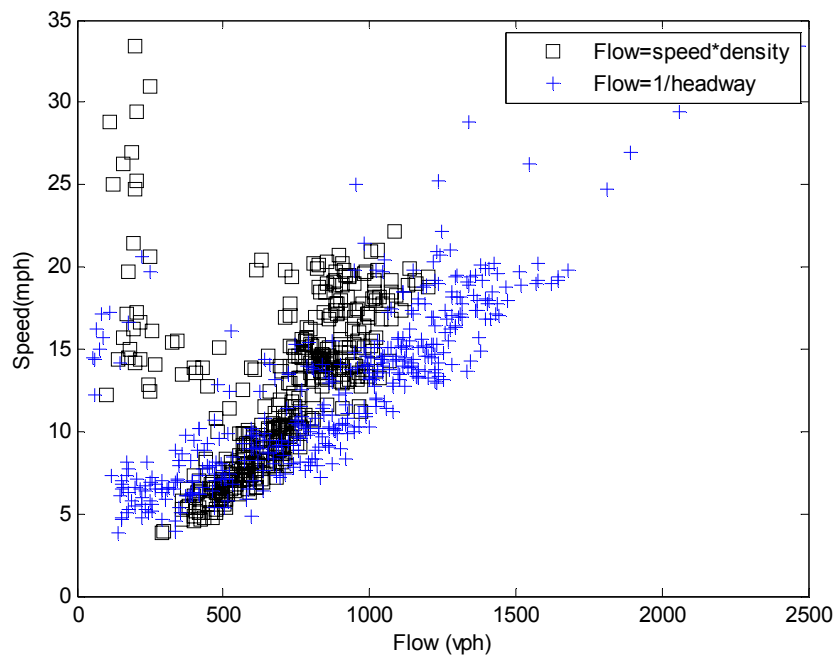


FIGURE 8 Speed Flow Plot for NGSIM Data using 2 Second Time Aggregation

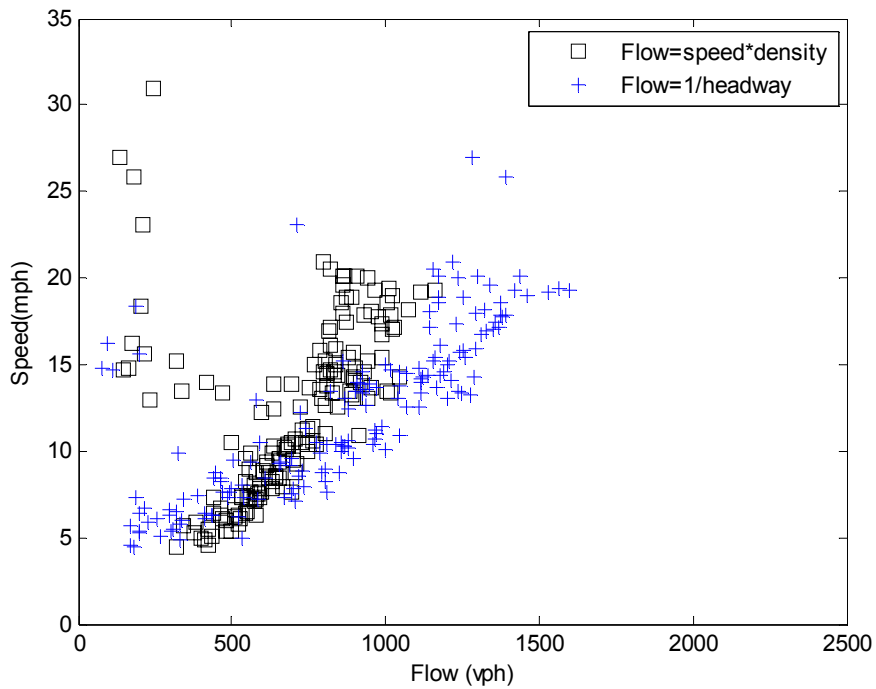


FIGURE 9 Speed Flow Plot for NGSIM Data using 5 Second Time Aggregation

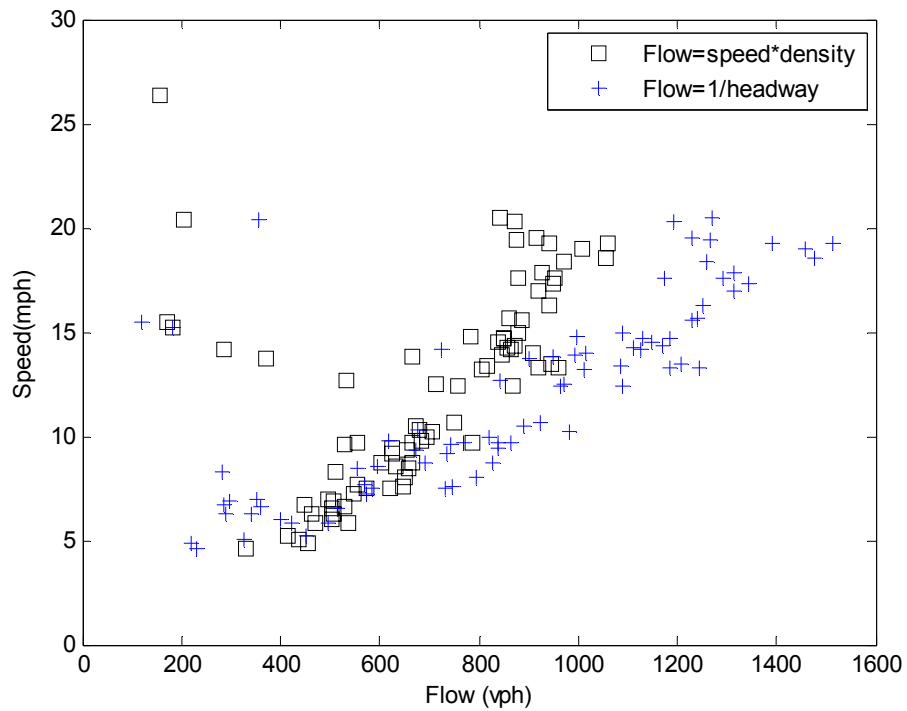


FIGURE 10 Speed Flow Plot for NGSIM Data using 10 Second Time Aggregation

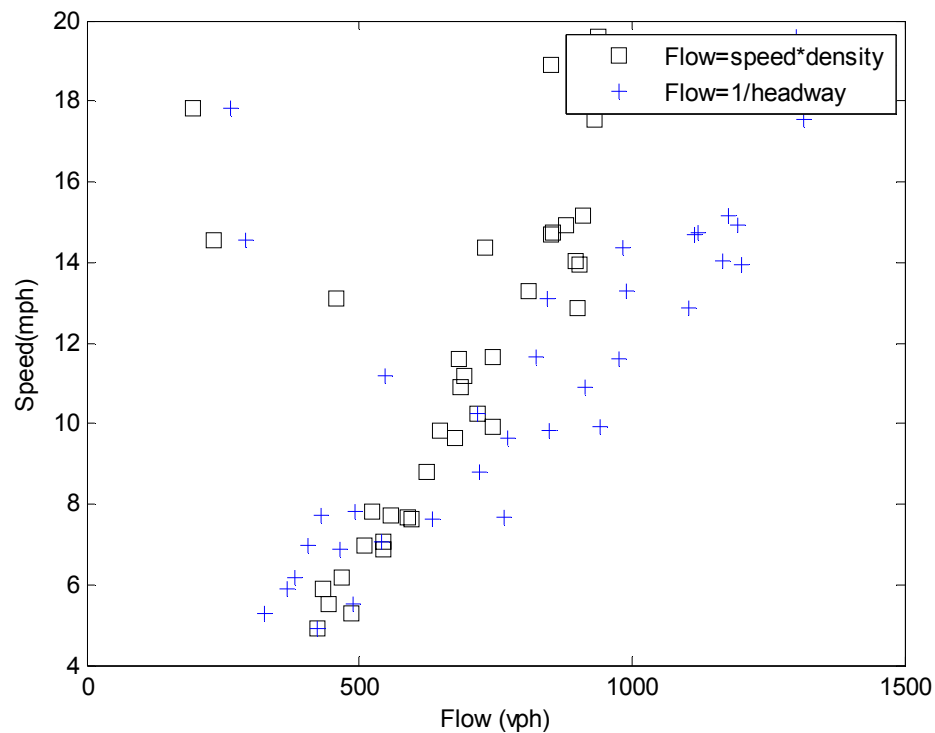


FIGURE 11 Speed Flow Plot for NGSIM Data using 20 Second Time Aggregation

5 APPLICATION OF THE CATASTROPHE THEORY

Catastrophe theory is typically applied in situations where a variable (state variable) can suddenly change its value while the other variables (control variables) show smooth changes. The state variable can also have smooth changes. As given by Zeeman (1977), the catastrophe is represented by the function which minimizes the potential function given in Equation 1(Zeeman 1977). The potential function has the critical surface defined by Equation 2.

$$W(X) = a X^4 + b U X^2 + c V X \quad \dots \dots \dots \text{Eq (1)}$$

where, X is the state variable

U and V are the control variables and

a, b and c are the parameters

$$4a X^3 + 2b U X + c V = 0 \quad \dots \dots \dots \text{Eq (2)}$$

The general shape of the cusp catastrophe surface and its three dimensional view generated as a part of this study is given in Figure 12.

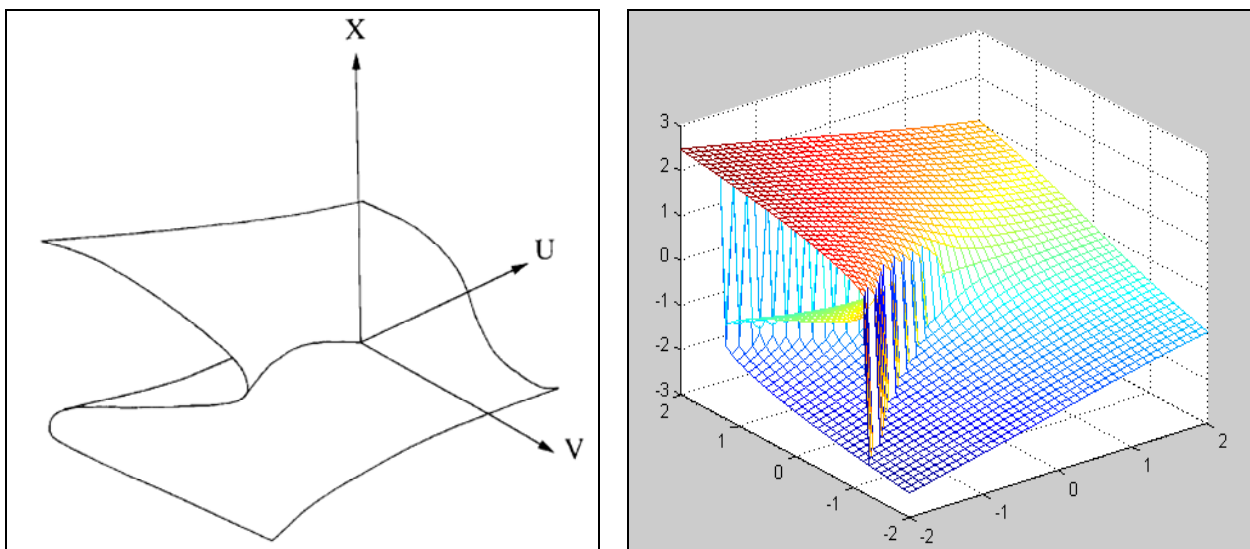


FIGURE 12 General Shape of Cusp Catastrophe Surface (Source: Acha-Daza, Hall, 1994) and its Three Dimensional View Created using Matlab

The middle part of the fold in Figure 12 represents the unstable (mathematically inaccessible) values of the state variable. They are the maxima of Equation 1 and they either do not occur or

are unstable in reality. Therefore, they change to stable values on the upper or lower sheets (Acha-Daza and Hall 1994). The projection of the fold on UV plane resembles a cusp, hence the name. Thus after removal of the middle portion of the fold, the state variable is expected to have two values in the cusp zone. However, due to some physical problems (in context of traffic flow the physical problems will be availability of space, traffic density, etc.), the state variable takes only one value in the cusp zone. For example, for a given flow value there may be two plausible speed values on the speed flow curve, however there will be only one speed value observed in field depending on the density of the traffic stream. In order to explain this behavior, two special conventions; Perfect Delay convention and Maxwell's convention are used. Hall (1987) suggested use of Maxwell's convention (Figure 13). In Maxwell's convention the upper and lower surfaces of in Figure 12 are separated by the vertical cut. The vertical cut lies on the U-axis ($V=0$). The transitions from one state to another occur instantaneously and the potential function always takes its global minimum.

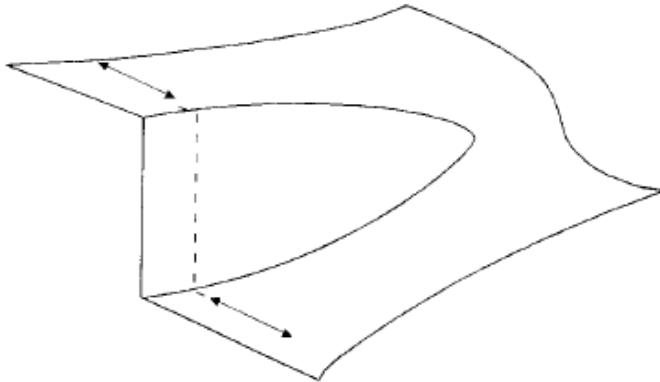


FIGURE 13 Maxwell's Convention for the Catastrophe Surface (Source Acha-Daza, Hall 1994)

Navin (1988) first suggested that the Catastrophe Theory can be applied to the traffic flow variables. Hall (1987) applied the theory to actual data. Speed was considered to be the state variable whereas flow and occupancy were considered to be the control variables. He suggested that it was necessary to transform these variables in order to represent the traffic data by the Catastrophe surface.

Data Transformation for Catastrophe Theory

The transformations are done in such a way that the origin in Figure 12 coincides with the traffic conditions at capacity. This is achieved by the axes translation which is given by (Acha-Daza and Hall 1994)

$$U_2 = \text{Volume} - \text{Maximum volume},$$

$$V_2 = \text{Occupancy} - \text{Maximum occupancy at maximum volume},$$

$$X_2 = \text{Speed} - \text{Minimum speed at maximum occupancy for maximum volume}$$

Theoretically, it is necessary that no data lie on the middle surface and the congested region data should be separated from the uncongested region data by the vertical cut (Maxwell's convention). In order to achieve this, axes rotation using equations 3 and 4 is necessary:

$$U = U_2 * \cos \theta - V_2 * Gf * \sin \theta \quad \dots \dots \dots \text{Eq (3)}$$

$$V = U_2 * \sin \theta + V_2 * Gf * \cos \theta \quad \dots \dots \dots \text{Eq (4)}$$

Where, Gf is a graphical factor. (in order to scale the data U and V),

$Gf = \text{Maximum volume} / \text{Maximum occupancy};$

The angle of axes rotation θ is found iteratively so as to minimize the number of points that are misclassified (points in the congested zone classified as uncongested zone points and vice versa). The critical speed value (minimum speed at the maximum occupancy for maximum volume) is used for the classification of the data point (congested or uncongested).

Calibration of the Catastrophe Model

Equation (2) is rewritten as Equation (5) by changing the parameters.

$$X^3 + a_1 * U * X + b_1 * V = 0 \quad \dots \dots \dots \text{Eq (5)}$$

Where $a_1 = 2b/4a$ and $b_1 = c/4a$

Hence calibration of Catastrophe model involves estimating the parameters a_1 and b_1 .

In Acha-Daza and Hall's approach for Calibration, Equation (3) was used to find the value of X . From this value of X the predicted speed can be calculated as:

$$Sp = X + \text{Minimum speed at the maximum occupancy for maximum volume} \dots \dots \dots \text{Eq (6)}$$

Since the expression is intrinsically linear (or nonlinear), use of a traditional linear regression analysis was not recommended. Instead, Acha-Daza and Hall used the direct search following the Hooke and Jeeves pattern search strategy to find the values of a_1 and b_1 . In this study we proposed alternate calibration technique based on Genetic algorithms.

Genetic Algorithm Approach for Calibration of the Catastrophe Model

This study proposed the use of genetic algorithm for calibration of the Equation (5). Readers are referred to Davis (1991) and Goldberg (1989) for basic concepts of Genetic Algorithms. The fitness function (the minimization function) was specified as the sum of squared difference between observed and predicted speeds for the sample. Equation (3) was solved in each step to find the value of X. Equation (5) is a cubic equation and it has one or three real roots. In case of three real roots, first the data point was classified as congested or uncongested depending on the value of V (transformed value of occupancy) and using the Maxwell's convention the predicted speed was calculated. If the value of V was less than or equal to zero, the data point was classified as the uncongested scenario and the largest (X) value among the three roots was used for calculation of the predicted speed. If the value of V was greater than zero it was classified as the congested scenario and the smallest speed value (X) among the three roots was used for calculation of the predicted speed.

The genetic algorithm starts with assumed values of a_1 and b_1 and calculates the sum of the squared difference between observed and predicted speeds. It then tries to minimize that value by changing values of a_1 and b_1 using the concepts in genetics and reproduction.

The I-35 loop detector data describe in the data section was used for studying the application of catastrophe theory. Using Hall's proposition for axes transformation the critical values used for transformation were as follows:

Maximum volume = 13 vehicles per 20 seconds

Maximum occupancy at maximum volume = 29 percent

Minimum speed at maximum volume and corresponding maximum occupancy = 23 miles per hour.

A Matlab code was written to transform the data for the Catastrophe theory and then to calibrate the Catastrophe model using Genetic Algorithms (Appendix A-2). The transformed volume and occupancy data is shown in Figure 14 and Figure 15. ($GF = 13/69$ (Maximum Volume / Maximum occupancy) Axes rotation by -16 degrees).

The predicted values versus actual speed values for this analysis are shown in Figure 16.

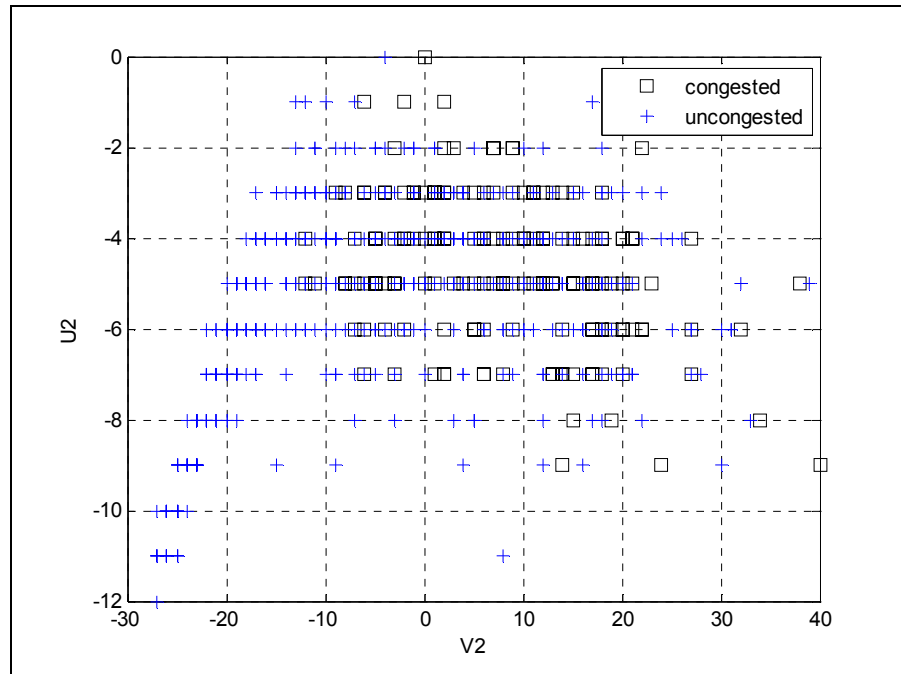


FIGURE 14 U2 (Volume) vs. V2 (Occupancy) following Axes Transformation

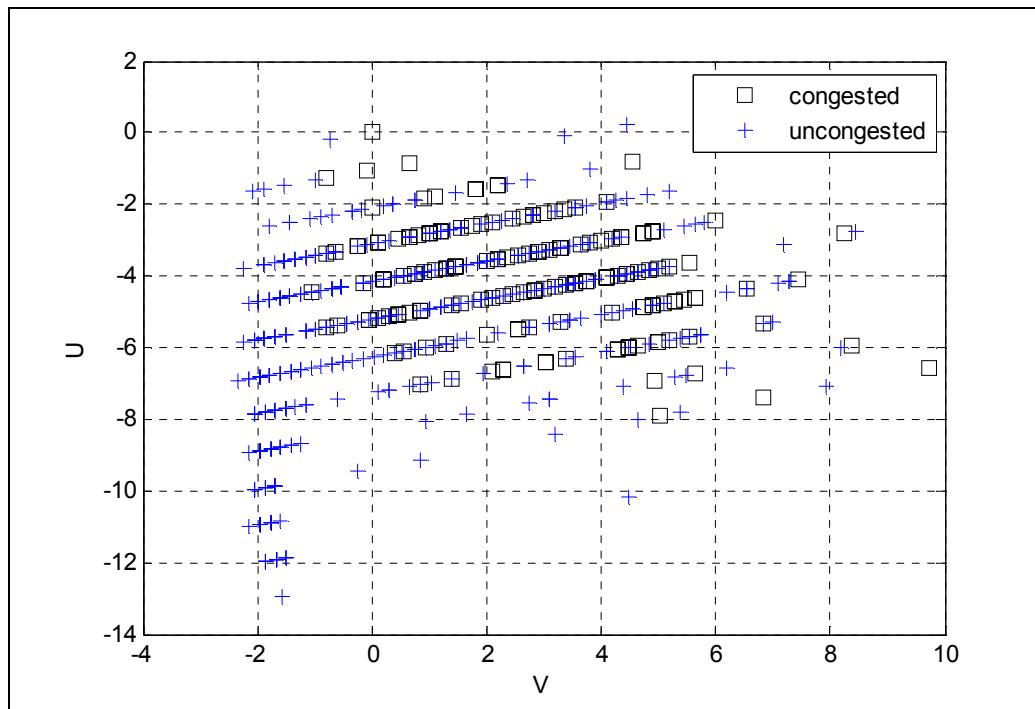


FIGURE 15 Volume vs. Occupancy data Following Graphical Transformation and Axes Rotation

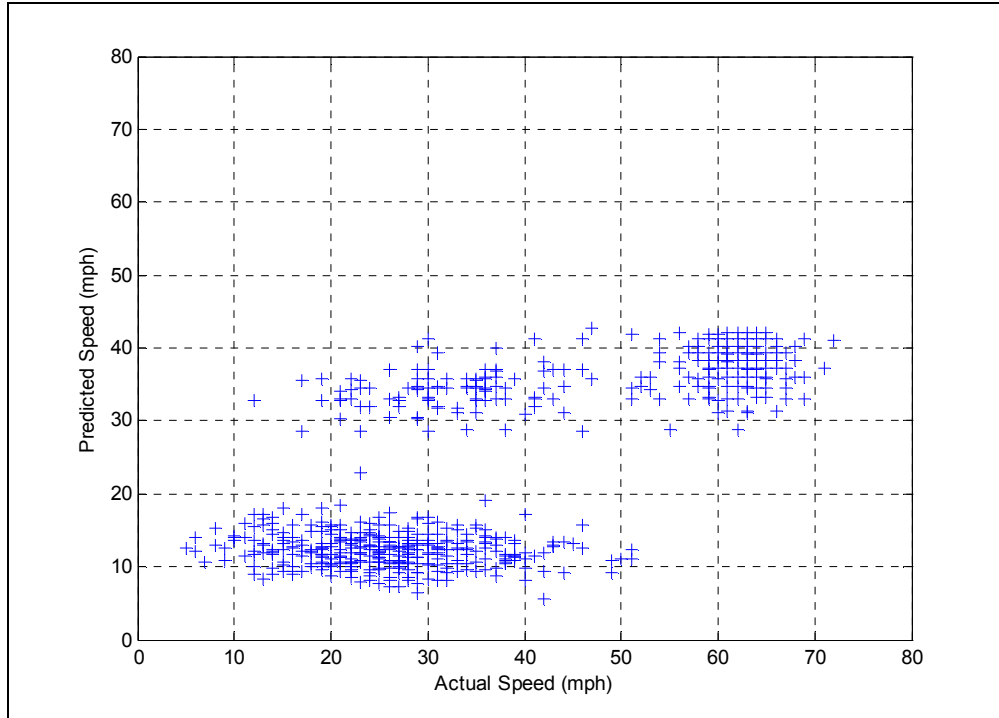


FIGURE 16 Prediction Success for Catastrophe Theory using Hall's Approach

The catastrophe theory model predicted speed values in only two ranges (Figure 16). The reason given by Hall for such behavior was the lack of equilibrium or the study location being located downstream of a bottleneck (hence having the queue discharge flow). Location of this data collection is 0.23 miles downstream of an entry ramp, hence it may be showing the characteristics of queue discharge flow.

Hall (1994) has also suggested that the Catastrophe model has a very high dependence on the critical values. The critical values were changed in order to estimate their effect on prediction success by trial and error. These values were then used for the calibration using the Genetic Algorithm. Following set of values were found to better classify the congested and uncongested data points during the transformation process.

Maximum volume = 13 vehicles per 20 seconds

Maximum occupancy at Maximum volume = 21 percent

Minimum speed at Maximum volume and corresponding Maximum occupancy = 40 mph

GF = 13/69 (Maximum volume / Maximum occupancy)

Axes rotation by -14 degrees.

The corresponding plots are given in Figure 17 and Figure 18. The prediction success is still very limited to two distinct groups of speeds as shown in Figure 19 and 20.

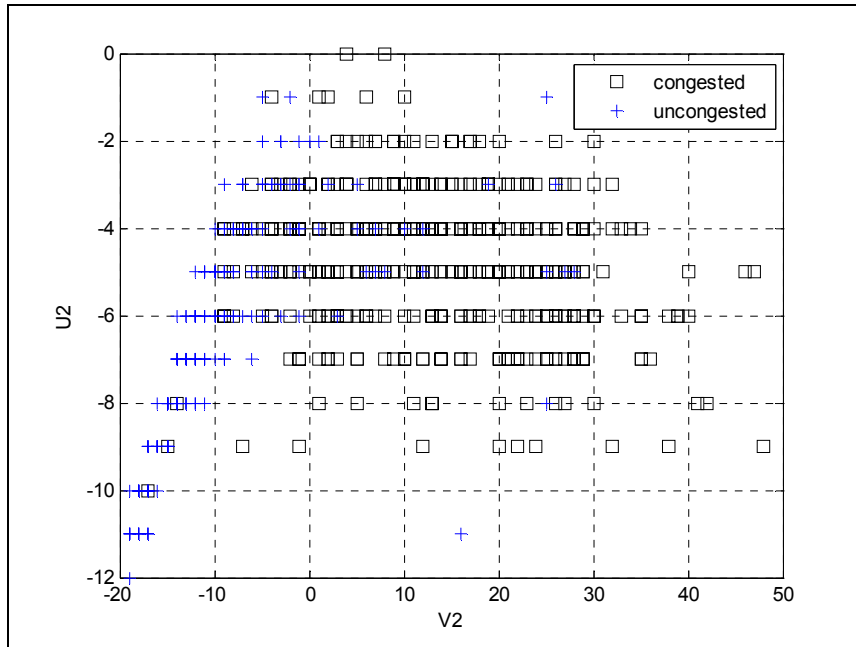


FIGURE 17 U_2 (Volume) vs. V_2 (Occupancy) following Axes Transformation using Trial and Error for Critical Values

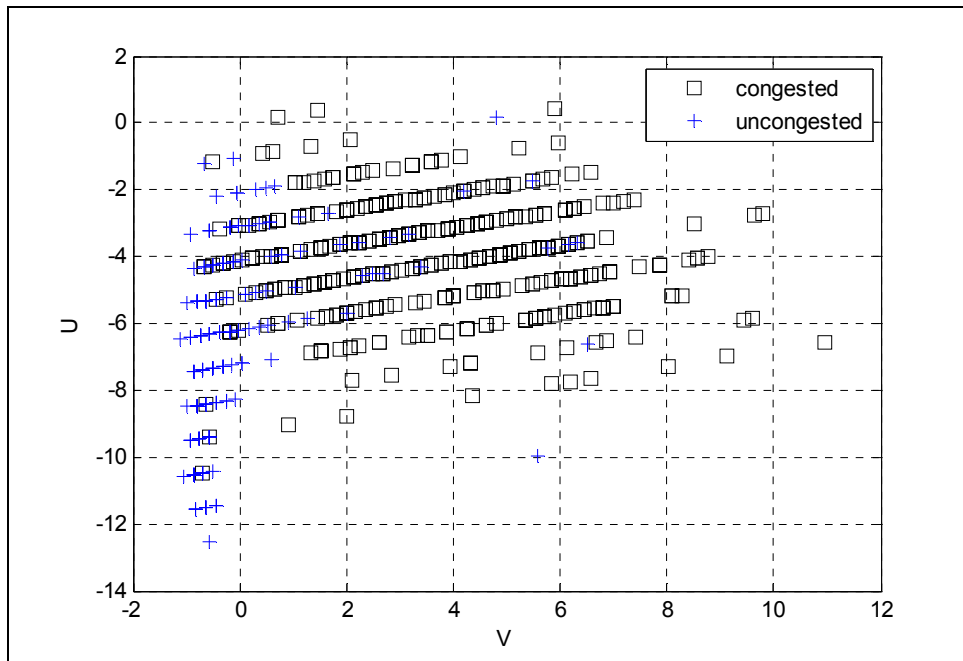


FIGURE 18 Volume vs. Occupancy Data Following Graphical Transformation and Axes Rotation Using Trial and Error For Critical Values

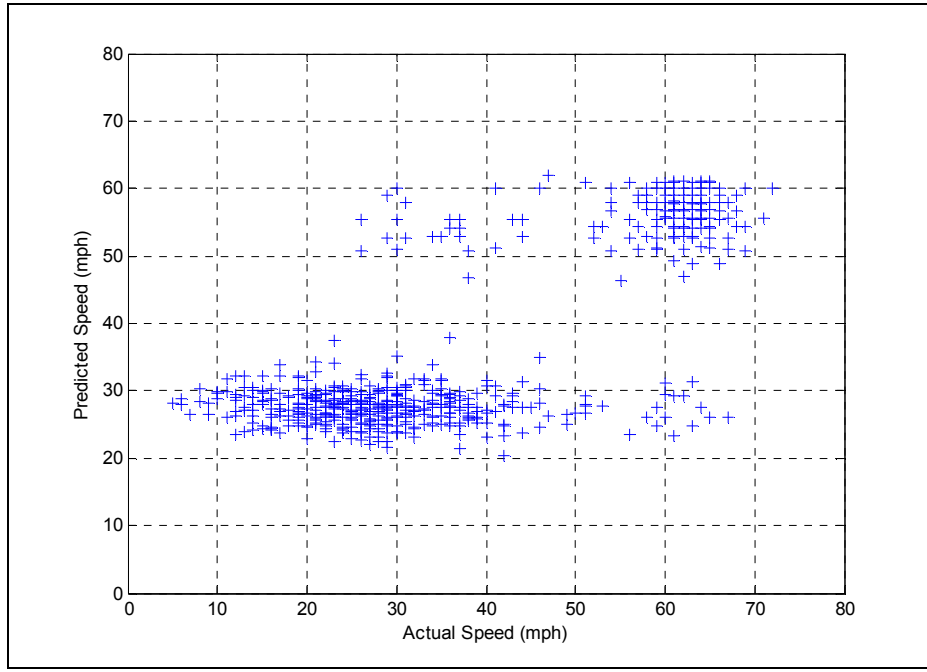


FIGURE 19 Prediction Success for Catastrophe Theory using Trial and Error for Critical Values

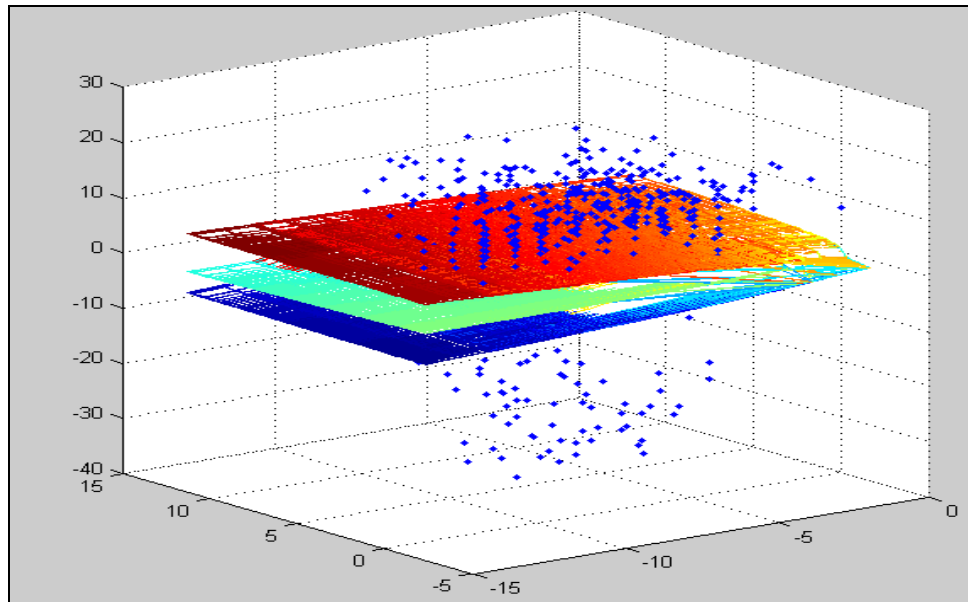


FIGURE 20 Three Dimensional Plot for the Prediction Success of Catastrophe Theory

The Wavetronix data was also used for this catastrophe application study which also yielded similar results (Figure 21) even though the location for this data collection is 0.21 miles

downstream of an exit ramp and 1.19 miles downstream of an entry ramp. Hence, having a queue discharge flow at this location is unlikely.

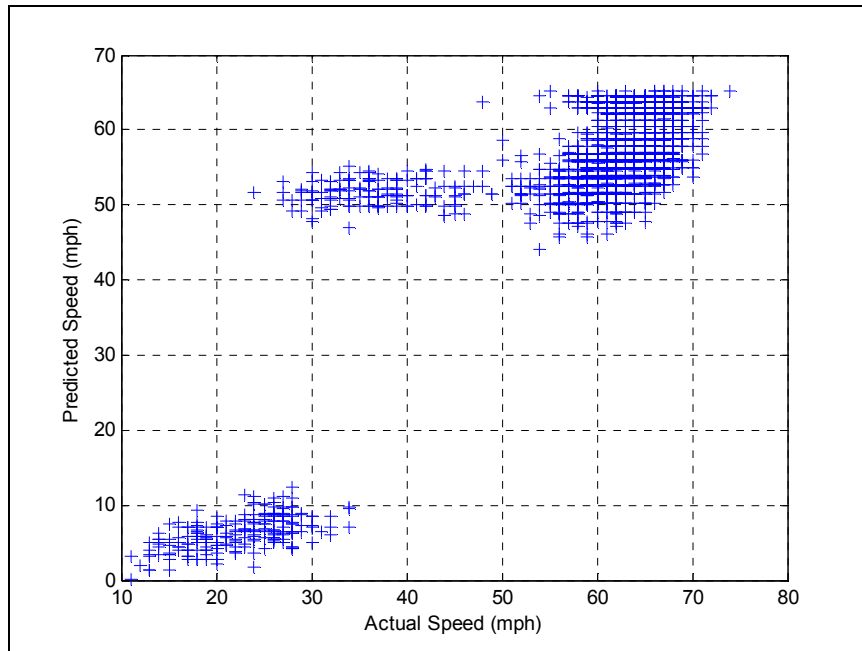


FIGURE 21 Prediction Success for Catastrophe Theory using I-45 Wavetronix Data

Apart from the possibility of queue discharge flow at very congested hours, the reason for the poor performance of Catastrophe Theory model is that it offers little flexibility in the calibration. The values of a_1 and b_1 play a vital role in the model prediction and as seen above it is very difficult to fit the model to the data only by specifying a_1 and b_1 . Also, these values of a_1 and b_1 are location and data set specific and its time consuming to estimate them every time for every data set. This increases the need of using a single-regime model with additional parameters (for adding some more flexibility). The Catastrophe model thus seems to be unsuitable for this study as it fails to predict the whole range of speeds.

6 APPLICATION OF MACROSCOPIC TRAFFIC FLOW MODELS

Previous literature has proposed many macroscopic traffic flow models (refer to May (1990) for an introductory discussion). In order to apply them to the theory of congestion pricing they need to be simple with few variables and at the same time they need to be accurate enough to predict the change in flow and speed near congestion. After a brief review of literature it was found that the models proposed by Li (2008) and Van Aerde (1995) may be applicable for this study (Van Aerde 1995).

Modified HCM Model

An additional parameter (α) extension to the HCM 2000 model was proposed by Li (2008) in order to extend it in the backward bending portion (hyper-congestion) of the speed-flow curve (with $V < V_o$). The speed-flow equation for this model was:

$$q = q_o \left(\frac{V}{V_o} \right)^\alpha \left(\frac{V_f - V}{V_f - V_o} \right)^{1/\beta} \quad \dots \dots \dots \text{Eq (7)}$$

Where, q_o = maximum flow level (veh/hr),

V_o = corresponding speed at q_o (km/hr),

V_f = free-flow speed (km/hr),

V = Speed (km/hr)

α and β are parameters such that $0 < \alpha \leq 1$ and $\beta > 0$. These parameters also they satisfy the condition in Equation 8 as given by Li (2008).

$$\frac{V_o}{V_f} = \frac{\alpha\beta}{(1+\alpha\beta)} \quad \dots \dots \dots \text{Eq (8)}$$

Therefore, α and β are related and knowing one implies the other. Hence the β value

$$\text{can be calculated as } \beta = \frac{\left(V_o / V_f \right)}{\alpha - \left(V_o / V_f \right) \alpha} \quad \dots \dots \dots \text{Eq (9)}$$

In order to find the optimum α value, the Mean Absolute Percentage Error (MAPE) analysis was used as the goodness of fit.

$$MAPE = \frac{\sum \frac{|actual - estimated|}{actual}}{\text{Number of Observations}} \times 100 \quad \dots \dots \dots \text{Eq (10)}$$

The actual speed values and estimated speed values for a model with an assumed α value were used for calculating MAPE using Equation 10. The MAPE values for various α values for data on April 14th 2006 are shown in Figure 22. After carrying out similar analysis for all 45 days data samples the average of optimum α values was found to be 0.39 (average MAPE was approximately 7 percent).

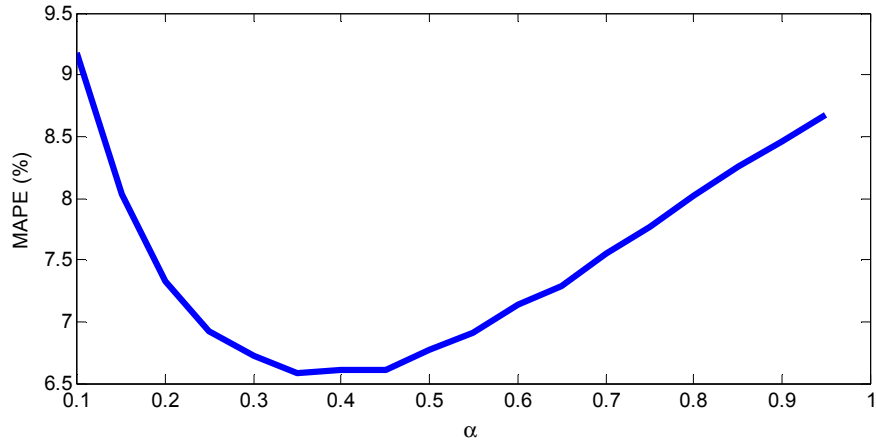


FIGURE 22 Optimum α Value for Modified HCM Model

Re-specified Newell-Franklin Model

Li (2008) re-specified the Newell-Franklin Model by replacing the variables, jam density and kinematic wave speed with optimum speed (V_o) and maximum flow (q_o) (Newell 1961, Franklin 1961). The functional form for this model is given by Equation 11,

$$q = q_o \left(\frac{V}{V_o} \right) \left(1 - \frac{1}{\beta} \ln \left(\frac{V_f - V}{V_f - V_o} \right) \right)^{-1} \quad \dots \dots \dots \text{Eq (11)}$$

where $\beta = \frac{V_o}{(V_f - V_o)}$, and other notation as specified earlier.

Using the values of $V_o=54$ mph (86.8 km/hr) and $V_f=64$ mph (102.9 km/hr) as obtained from the capacity analysis in Chapter 4, the β value was calculated to be

$$\beta = \frac{86.8}{(102.9 - 86.8)} = 5.4.$$

Van Aerde Model

Van Aerde proposed a steady state car following model with multiple parameters as given below (Aerde and Rakha 1995). The speed-flow equation is given by Equation 12,

$$q = \frac{V}{c_1 + \frac{c_2}{(V_f - V)} + c_3 V} \quad \dots \dots \dots \text{Eq (12)}$$

$$\text{where, } c_1 = mc_2, m = \frac{2V_o - V_f}{(V_f - V_o)^2}, c_2 = \frac{1}{k_j(m + (1/V_f))}, c_3 = \frac{-c_1 + \frac{V_o}{q_o} - \frac{c_2}{V_f - V_o}}{V_o}, \text{ and other}$$

notation as specified earlier.

The jam density value k_j was assumed to be 110 veh/km which gave good fit for the data. Also, using the values of V_o , q_o and V_f as obtained in the capacity analysis in Chapter 4 the values of c_1 , c_2 and c_3 were calculated as

$$m = \frac{2 * 86.8 - 102.9}{(102.9 - 86.8)^2} = 0.27276, c_2 = \frac{1}{110(0.27276 + (1/102.9))} = 0.032,$$

$$c_1 = mc_2 = 0.2727 * 0.032 = 0.0088,$$

$$c_3 = \frac{-c_1 + \frac{V_o}{q_o} - \frac{c_2}{V_f - V_o}}{V_o} = \frac{-0.0088 + \frac{102.9}{1684} - \frac{0.032}{102.9 - 86.8}}{86.8} = 0.0005$$

Application of the Data

The models above were compared to the real world data (I-45 dataset described in Chapter 3) using the values estimated in the capacity analysis. The data and predicted values are shown in Figure 22. All three models, the Modified HCM, Newell Franklin and Van Aerde models fit the uncongested to moderately congested region well. Further all three models predict similar values of flow and speed for the uncongested to moderately congested region. Modified HCM and Van Aerde models over predict the speeds in the hyper-congested region of speed flow diagram. However, the goal of congestion pricing is to avoid extreme congestion. Therefore, models that accurately predict speed and flow up to the congested region can be used for this research.

Comparison with Vickery's Bottleneck Model

Vickery's Bottleneck model as described in Chapter 2, has been widely used in the congestion pricing literature to estimate schedule delay costs and marginal costs of travel on congested roadways (Vickery 1969, Braid 1996, Arnott et. al 1990, Arnott and Kraus 1993, Cohen 1987, Chu 1993, Daganzo 1985, Small 1992). This study compares the speeds predicted by using the bottleneck model with the actual speed-flow data (Figure 23). The speed-demand curve for the bottleneck model seems to fit the free flow conditions; however as the traffic flow approaches the capacity the bottleneck model still predicts the same speed (FFS). This is unrealistic when compared with the field observations and hence the bottleneck model does not seem to represent the data well near the capacity. The Bottleneck model predicts unrealistic speeds when the demand exceeds the capacity.

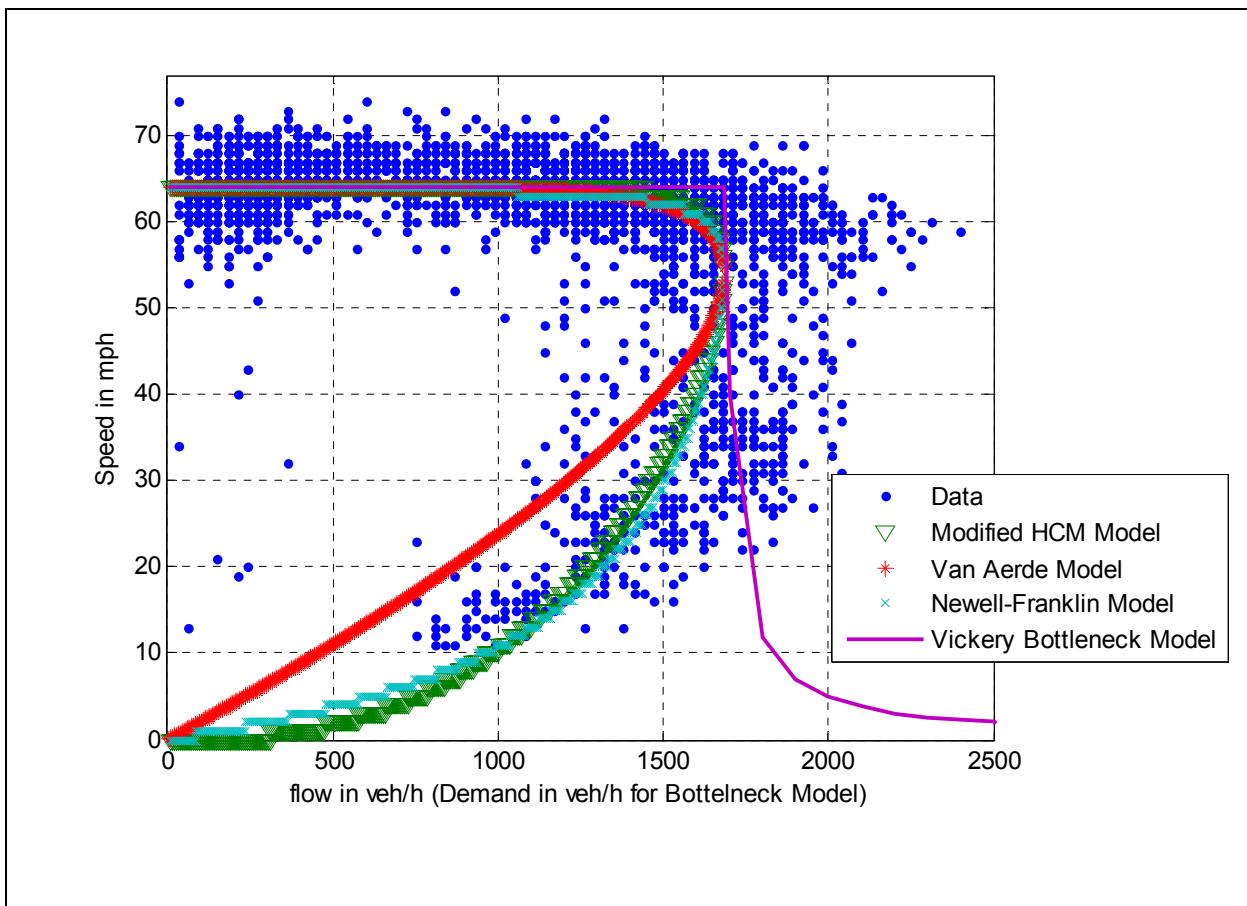


FIGURE 23 Application of Selected Traffic Flow Models to Data

Hence the Modified HCM model, Van Aerde Model and Newell Franklin models were used to develop a toll price for congestion pricing.

7 APPLICATION OF CONGESTION PRICING THEORY

The goal of congestion pricing is to price travel at its marginal social cost. When a highway nears capacity this cost increases rapidly such that travelers choose not to use the highway at that time. This would prevent the highway from becoming hypercongested. Thus our focus is on the upper section of the speed flow curve, where the speed is greater than or equal to the optimum speed at the capacity ($V \geq V_o$). The optimum toll rate can be estimated as explained below.

The flow q can be considered as a function of speed V ,

$$q = q(V)$$

Assuming the length of section under consideration as $d = 1$ km (hence the travel time to be 1/speed that is $1/V$) and the generalized cost (including value of travel time savings) as c \$/hr we can write the average cost (AC) to a traveler as the product of the travel time and the generalized cost,

$$AC(q) = c/V \text{ (per km)}$$

The total cost to q vehicles will be given by multiplying the AC by the flow q ,

$$TC(q) = (qc)/V \text{ which gives the marginal cost as}$$

$$MC(q) = \frac{dTC(q)}{dq} = \frac{d(\frac{qc}{V})}{dq}$$
$$MC(q) = \frac{c}{V} \left(\frac{dq}{dq} \right) - \frac{qc}{V^2} \left(\frac{dV}{dq} \right) = AC(q) - \frac{qc}{V^2} \left(\frac{dV}{dq} \right)$$

For an optimal toll the congestion toll (r) must be equal to the difference in marginal cost and average cost to the traveler.

$$r = -\frac{qc}{V^2} \frac{dV}{dq} \quad \dots \dots \dots \text{Eq (13)}$$

Using Equation 13 we can find the congestion toll estimation expressions for various traffic flow models. Li (2008) gives the equation for modified HCM and re-specified Newell-Franklin models.

The congestion toll estimation for Modified HCM Model

$$r = \left(\frac{c}{V} \right) \left(\frac{V_o - (\alpha\beta/(1+\alpha\beta))V}{\alpha(V - V_o)} \right) \quad \dots \dots \dots \text{Eq (14)}$$

Congestion toll Estimation for Re-specified Newell-Franklin Model

$$r = \frac{c}{V} \frac{1 - \frac{1}{\beta} \ln(\frac{V_f - V}{V_f - V_o})}{\frac{V}{V_o} \frac{V_f - V_o}{V_f - V} - 1 + \frac{1}{\beta} \ln(\frac{V_f - V}{V_f - V_o})} \quad \dots \dots \dots \text{Eq (15)}$$

The congestion pricing toll estimate can be easily derived for the Van Aerde model as follows:

$$r = -\frac{qc}{V^2} \frac{dV}{dq} = -\frac{qc}{V^2} \left[\frac{1}{dq/dv} \right]$$

Using the flow equation for Van Aerde model given in Eq (12) and taking the inverse of its derivative with respect to the speed (V) we get dv/dq

$$\frac{dv}{dq} = \left(c_1 + \frac{c_2}{(V_f - V)} + c_3 V \right)^2 \frac{1}{\left[c_1 + \frac{c_2}{(V_f - V)} - \frac{c_2 V}{(V_f - V)^2} \right]}$$

Hence,

$$r = -\frac{c}{V} \frac{\left(c_1 + \frac{c_2}{(V_f - V)} + c_3 V \right)}{\left[c_1 + \frac{c_2}{(V_f - V)} - \frac{c_2 V}{(V_f - V)^2} \right]} \quad \dots \dots \dots \text{Eq (16)}$$

where c is the generalized cost mentioned above.

Calculation of Toll Rates

These macroscopic traffic flow models were used to find the marginal cost of congestion. Finding the marginal cost was equivalent to finding the difference in the optimal tolls for traffic flow before and after an additional vehicle joins the traffic stream. Using Equations 14, 15 and 16 the toll for a given traffic speed was calculated. The traffic flow models were used to find the speeds for the given flows which were then substituted in to the toll estimation equations to find the optimal tolls. Matlab code was written to find the speed from the flow and is given in

Appendix A-3. The code written predicts both uncongested and congested speeds, only uncongested region speeds were used for toll estimation. The value of operating cost including the (fixed) value of travel time savings was assumed to be \$20/hr (The USDOT guidelines specify the Value of Travel Time Savings (VTTS) can vary between 20 to 30 \$/hr (USDOT 2003)) The code written can be used to increase the flow just by one vehicle/hr. The optimal toll rates estimated for various flows are shown in Figure 24 and Figure 25.

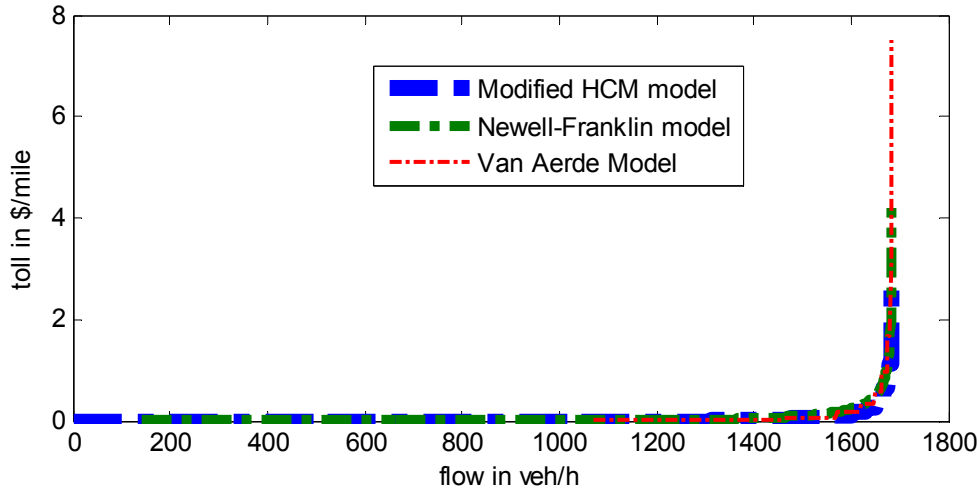


FIGURE 24 Congestion Toll Estimation for Various Traffic Flow Models at Different Flow Levels

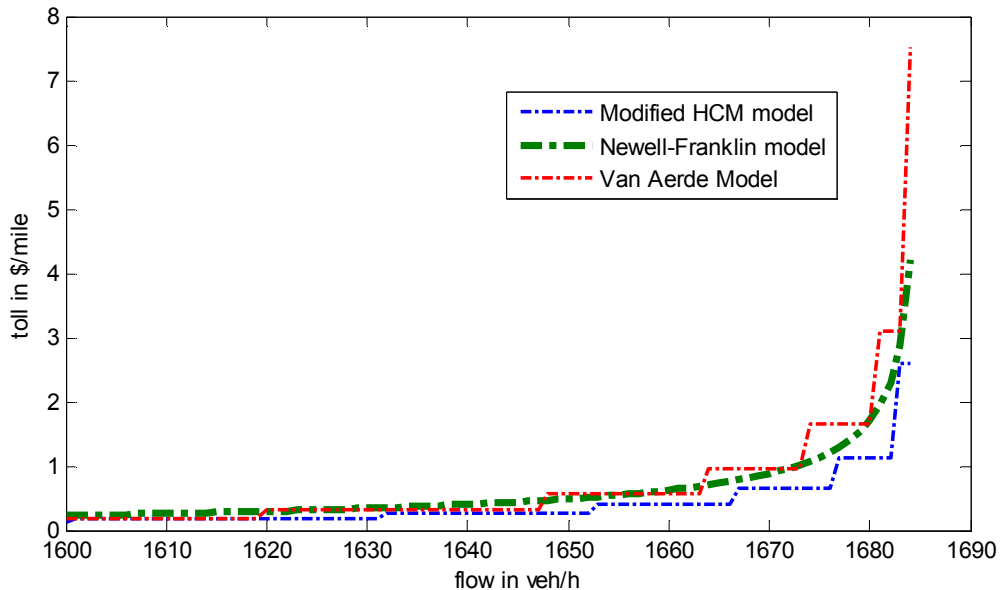


FIGURE 25 Congestion Toll Estimation for Near Capacity Flow Values for Various Traffic Flow Models

Sensitivity of Toll Estimation to the Value of Capacity

Capacity is one of the variables that enter the speed flow relation and hence the toll calculations. The capacity value is dependent on many factors and is different for different sections of the roadway. Hence the effect of the value of capacity on the toll estimation was studied. Different capacity values were used to calculate the optimal toll rates for different flows. Flows equal to 99%, 95%, 90%, 85% and 80% of several capacity values were used in the calculations (see Table 3). It can be observed that the modified HCM model and the Newell-Franklin model were not sensitive to the capacity of the roadway (See Figure 26) since the toll rate equations, Equation 13 and 14 are not dependent on the capacity (the parameters α and β also don't depend on capacity value). For the Van Aerde model the estimated toll rate decreases as the capacity value increases since the parameter c_3 used in the toll rate estimation (see Equation 14) depends on the value of capacity.

TABLE 3 Sensitivity of Toll Estimation for Assumed Capacity Values

Modified HCM		Toll Rates for				
Capacity Value q_o (veh/hr)	99% of q_o	95% of q_o	90% of q_o	85% of q_o	80% of q_o	
1600	0.651	0.177	0.064	0.028	0.028	
1685	0.651	0.177	0.064	0.028	0.028	
1700	0.651	0.177	0.064	0.028	0.028	
1750	0.651	0.177	0.064	0.028	0.028	
1800	0.651	0.177	0.064	0.028	0.028	
1900	0.651	0.177	0.064	0.028	0.028	
2000	0.651	0.177	0.064	0.028	0.028	
Newell-Franklin		Toll Rates for				
Capacity Value q_o (veh/hr)	99% of q_o	95% of q_o	90% of q_o	85% of q_o	80% of q_o	
1600	0.814	0.235	0.110	0.061	0.035	
1685	0.814	0.235	0.111	0.061	0.035	
1700	0.814	0.235	0.110	0.061	0.035	
1750	0.814	0.235	0.110	0.061	0.035	
1800	0.814	0.235	0.110	0.061	0.035	
1900	0.814	0.235	0.110	0.061	0.035	
2000	0.814	0.235	0.110	0.061	0.035	
Van Aerde		Toll Rates for				
Capacity Value q_o (veh/hr)	99% of q_o	95% of q_o	90% of q_o	85% of q_o	80% of q_o	
1600	1.016	0.177	0.076	0.021	0.021	
1685	0.965	0.169	0.073	0.020	0.020	
1700	0.957	0.167	0.072	0.020	0.020	
1750	0.930	0.163	0.071	0.019	0.019	
1800	0.904	0.159	0.069	0.019	0.019	
1900	0.857	0.151	0.065	0.018	0.018	
2000	0.815	0.144	0.063	0.017	0.017	

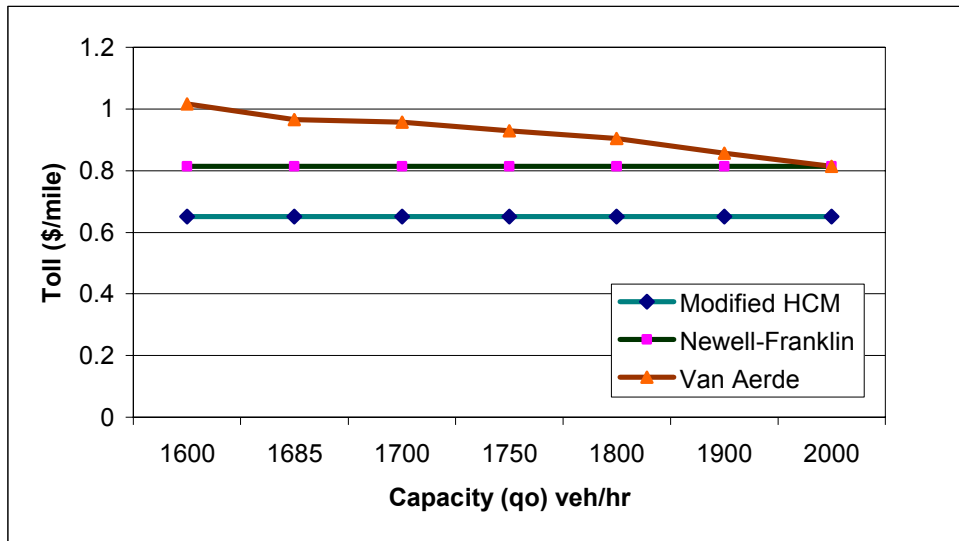


FIGURE 26 Effect of Capacity Value on the Toll Rate Estimation for Flow Equal to 99 percent of Capacity

Comparison of the Optimum Toll Rates with Toll Rates on Existing Variable Priced Toll Lanes

This study compares the optimum toll rates found in the previous section with the current toll rates on the SR-91 Express lanes in California, SR-167 HOT (High Occupancy Toll) lanes in Washington and I-15 Express Lanes in San Diego.

The toll rates on SR-91 Express lanes in Orange County, California vary every hour. The current tolls (October 2008) on the SR-91 Express lanes vary from \$0.125/mile in off-peak hours to \$0.95/mile in peak of peak hour (Orange County Transportation Authority 2008). SR-167 HOT lanes in the Washington State are dynamically priced where the toll rate varies dynamically in order to keep the speed of vehicles on the HOT lanes over 45 miles per hour. On SR-167 HOT lanes, the toll rates vary from \$0.056/mile at off-peak hours to \$1/mile at peak hours (WSDOT 2008). Toll rates on I-15 Express lanes in San Diego vary every six minutes to maintain the speed of 60 mph. The toll rates vary from \$0.06/mile to \$1.00/mile (when the congestion is very severe) depending on the traffic volume (SANDAG 2008). The comparison of toll rates on these facilities with the optimum toll rates estimated in this study is shown in Table 4. The maximum real world toll rates are in the same range as the ones calculated here. However, since the optimum toll rates vary based on the assumed generalized cost of travel per hour, this variable needs added study for estimation of a specific congestion pricing toll on a given route. Also, it should be noted that the marginal cost starts exceeding the average cost (approximately) when

the flow starts increasing beyond 70% of the capacity. Hence the optimum toll rate for free flow and lower flow conditions is zero when calculated using any of the models mentioned above.

TABLE 4 Comparison of Toll Rates on SR-91 and SR-167 with the Optimum Toll Rates

Traffic Flow Model	Flow near capacity (1684 veh/hr)			Free Flow (<500 veh/hr) Conditions		
	Optimum Toll Rates (\$/mile) for different Generalized Travel Costs (GTC)			Optimum Toll Rates (\$/mile) for different Generalized Travel Costs (GTC)		
	GTC =\$20/hr	GTC =\$30/hr	GTC =\$40/hr	GTC =\$20/hr	GTC =\$30/hr	GTC =\$40/hr
Modified HCM Model	0.65	0.98	1.30	0	0	0
Newell-Franklin Model	0.81	1.22	1.63	0	0	0
Van Aerde Model	0.97	1.45	1.93	0	0	0
Maximum toll rate on SR-91, California (November 2008)	\$0.95/mile			\$0.125 /mile		
Maximum toll rate on SR-167, Washington (November 2008)	\$1/mile			\$0.056 /mile		
Maximum toll rate on I-15, San Diego (till August 2008)	\$1/mile			0.06		

8 CONCLUSIONS

This study examines traffic data from various sources collected using different technologies (such as loop detectors, radars and video) to estimate the impact of additional vehicles near capacity. A detailed analysis was carried out to study the variation in the capacity values of the freeway section under consideration. Also, the critical values for traffic flow models such as free flow speed and speed at the capacity were estimated. For I-45 freeway in Houston the free flow speed was found to be 64 miles per hour and the capacity was found to be 1684 vehicles per hour for the study location. The corresponding speed at the capacity was found to be 54 miles per hour.

Two of the data sets were used to test the applicability of the Catastrophe Theory to the traffic flow variables speed and flow. An innovative approach for calibrating the intrinsically linear Catastrophe model using Genetic Algorithms was developed. The Catastrophe theory was found to be of limited use as it predicted speeds in only two groups. The prediction success of the Catastrophe model was found to be affected largely by the location of the data collection and the calibration parameters. Hence it was not used for further analysis of the congestion pricing. Unlike the Catastrophe model, three macroscopic traffic flow models were found to provide a good fit to the available data. The Modified HCM model, Newell-Franklin model and the Van Aerde model all provided an excellent fit in the upper section of the speed flow curve. Further these models provided a better fit to near capacity and hyper-congested region than the Vickery's bottleneck model. The bottleneck model estimated the free flow speed for all the flow values ranging from free flow conditions to the capacity, which is not realistic. Also, it performed poorly in estimating the speeds for conditions when the demand exceeds the capacity.

The Modified HCM model, Newell-Franklin model and the Van Aerde model were then used to calculate the optimum congestion toll estimates using the theory of congestion pricing. All three models gave similar toll rate estimates up to flow equal to 95 percent of the capacity. Unlike Modified HCM and Newell-Franklin models, the toll rate estimation for Van Aerde model was found to depend on the capacity value used for specifying the model.

Further these optimum toll rates were compared to the current (October 2008) toll rates on SR-91 in California, I-15 in San Diego and SR-167 in Washington. The current toll rates on

SR-91, I-15 and SR-167 are higher when compared with the optimum toll rates calculated in this study using the generalized travel cost of \$20 per hour but they are lower when compared with the optimum toll rates calculated using the generalized travel cost of \$40 per hour. Apart from the generalized travel cost, the optimum toll rates also depend highly on the traffic flow model used. The Modified HCM model yielded lowest optimum toll rates while the Van Aerde model yielded highest optimum toll rates. The toll rates estimated using Van Aerde model were found to be close to the current toll rates on above facilities. However, it should be noted that the facilities mentioned above are High Occupancy Toll (HOT) lane type of facilities, where carpoolers (two or more travelers in a vehicle) receive discount (up to 100%) in toll rates and the toll rates described here are paid only by the Single Occupant Vehicles (SOVs). Hence, it can be said that a percentage (or the class) of vehicles are charged with the whole marginal cost. It will be worth studying this type of facility from congestion pricing theory point of view as a future extension of this work.

REFERENCES

1. Acha-Daza, J.A. and Hall, F.L., The Application of Catastrophe Theory to Traffic Flow Variables. *Transportation Research Record* 28B, pp. 235–250, 1994
2. Aerde, M., and H. Rakha Multivariate Calibration of Single Regime Speed-Flow-Density Relationships. Proceedings of the 6th *Vehicle Navigation and Information System Conference* (VNIS), Seattle, WA, IEEE, Piscataway, NJ, pp.334-341, 1995.
3. Aerde, Van, M. A Single Regime Speed-Flow-Density Relationship for Freeways and Arterials. Presented at 74th Annual Meeting of the Transportation Research Board, Washington, D.C., 1995.
4. Arnott, R.J., A. de Palma, and R. Lindsey, Economics of a bottleneck, *Journal of Urban Economics*, 27, pp.111-130,1990.
5. Arnott R.J. and M. Kraus, The Ramsey problem for congestible facilities, *Journal of Public Economics*, 50, pp.371-396, 1993.
6. Banks, J.H, An investigation of some characteristics of congested flow, *Transportation Research Record* 1678, pp.128–134, 1999
7. Banks, J.H. Review of Empirical Research on Congested Freeway Flow, *Transportation Research Record* 1802,pp.252-232,2002.
8. Bassan, S. Modeling Traffic Flow Transition and Breakdown Processes on Congested Freeways, PhD Dissertation, University of Delaware, 2005.
9. Braid, R.M, Peak-load Pricing of a Transportation Route with an Unpriced Substitute, *Journal of Urban Economics*, 40, pp. 179-197, 1996.
10. Carter and Burgess, Inc, I- 35 San Antonio Northeast Corridor Traffic Report. Disk 1 of 1, Carter and Burgess, Inc, Austin, TX, November 2002.
11. Chu, X., 1993. Trip Scheduling and Economic Analysis of Transportation Policies. Unpublished Ph.D. dissertation, University of California, Irvine, Department of Economics.
12. Cohen, Y. Commuter welfare under peak-period congestion tolls: Who gains and who loses?, *International Journal of Transport Economics*, 14, pp.238-266,1987.
13. Daganzo, C.F. The uniqueness of a time-dependent equilibrium distribution of arrivals at a single bottleneck, *Transportation Science*, 19, pp.29-37,1985.
14. Davis L, *Handbook of Genetic Algorithms*. Van Nostrand Reinhold, New York, 1991

15. Franklin, R. E. The Structure of a Traffic Shock Wave, *Civil Engineering Public Works Review*, Vol. 56, pp. 1186-1188, 1961.
16. Goldberg, D.E. Genetic Algorithms in Search Optimization and Machine Learning, Addison Wesley, Reading, PA, 1989.
17. Greenberg, H., An Analysis of Traffic Flow, *Operation Research* 7, 1959.
18. Hall, F., An Interpretation of Speed-Flow Concentration Relationships using Catastrophe Theory. *Transportation Research* A 21, pp.191-201, 1987.
19. Highway Capacity Manual: HCM2000. Transportation Research Board, NRC, Washington, DC, 2000.
20. Li, Michael Z. F.A Generic Characterization of Equilibrium Speed-Flow Curves *Transportation Science* 42, pp. 220-235, 2008.
21. MATLAB User's Guide, The Math Works Inc., Natick, 1994.
22. May, A.D. *Traffic Flow Fundamentals*. Prentice Hall, Upper Saddle River, NJ, 1990.
23. Navin, F.D, Traffic Congestion Catastrophes, *Transportation Planning and Technology* 11,pp.19-25, 1988
24. Newell, G.F. Nonlinear Effects in the Dynamics of Car-following, *Operation Research* 9, pp.209-229, 1961.
25. NGSIM Homepage. FHWA. <http://ngsim.fhwa.dot.gov>.
26. Orange County Transportation Authority, Toll Schedules on SR-91 Express Lanes <http://www.91expresslanes.com/tollschedules.asp>. Last Accessed November 10, 2008.
27. Polus A. and Pollatschek M., Stochastic Nature of Freeway Capacity and its Estimation. *Canadian Journal of Civil Engineering* 29. 842-852, 2002.
28. San Diego Association of Governments (SANDAG) website, http://fastrak.511sd.com/PDFs/I-15_FactSheet_001.pdf, Accessed on November 11, 2008.
29. Small, K.A., Trip scheduling in urban transportation analysis, *American Economic Review, Papers and Proceedings*, **82**, pp. 482-486,1992.
30. USDOT, Revised Departmental Guidance: Valuation of Travel Time in Economic Analysis. U.S. Department of Transportation, Feb. 2003.

31. Vickery, W.S. Congestion Theory and Transport Investment, *American Economic Review* (Papers and Proceedings), 59, pp.251-260, 1969.
32. Walters, A.A., The theory and Measurement of Private and Social Cost of Highway Congestion. *Econometrica* 29 , pp. 676–699, 1961.
33. Washington State Department of Transportation, Toll Rates on SR-167,
<http://wsdot.wa.gov/goodtogo/tollrates>
34. Zeeman, E. C., 1977, *Catastrophe Theory: Selected Papers, 1972-1977* (Addison-Wesley, London).
35. Zhou, M. and F.L. Hall, Investigation of Speed-Flow Relationship Under Congested Conditions on a Freeway. *Transportation Research Record*, pp.64-72, 1999.

APPENDIX A-1

```
% start with the data within selected 200 feet section
dtmtrx=[VehID FRID Nframes GlbTime Local_X Local_Y Global_X Global_Y VehLen
VehWidth VehClass Veh_Vel Veh_Acc Lane_ID Prec_Veh Fol_Veh SHeadway
THeadway];
% above statement combines the vectors in a single matrix for data analysis

outliers1 = dtmtrx(:,6)>200; % width of the section,.. original width 200
(Y=0 to Y=200)
*****change the value 200 at line 117 in density calculation
dtmtrx(any(outliers1,2),:)= [];

%delta_t is the time aggregation value
delta_t=2;%***** Change delta-t
here*****
Ts=1113433139; % tmin=1113433135300 milisec 1113433335.300 *****change for
differenet data set***

dts=NaN(50,1);
nv=NaN(50,1);
avgd=NaN(50,1);
sumtt=NaN(50,1);avgtt=NaN(50,1);tms=NaN(50,1);SMS=NaN(50,1);
avgHa=NaN(50,1);flowh=NaN(50,1);
flowd=NaN(50,1); density=NaN(50,1);

% Now remove those vehicles having time headway=0 i.e. the vehicles present
at
% the begining of the study.
outliers = dtmtrx(:,12)==0;
%similar variable( outlier) can be created for differenct lengths of the
%section based on Local_Y variable
dtmtrx(any(outliers,2),:)= [];
%Here, any(outliers,2) returns a 1 when any of the elements in the outliers
%vector is a nonzero number, and the argument 2 specifies that any works
%down the second dimension of the count matrix – its columns.

mtx=dtmtrx;
k=1; % counter for time increment.. t,t+delta_t, t+2delta_t... (speed
flow,density for each time period
while ((Ts+delta_t)<=(1113434083800/1000)&&length(dtmtrx(:,1)>0))
***** delta-t here*****
dtmtrx=mtx; % nullifies the changes made in dtmtrx in previous iterations
outliers2=((dtmtrx(:,4)/1000)>(Ts+delta_t))|((dtmtrx(:,4)/1000)<Ts));
***** delta-t here*****
%select the delta_t sec time window and reject other data
dtmtrx(any(outliers2,2),:)= [];
if length(dtmtrx)>1
nveh=length(unique(dtmtrx(:,1)));% to count the no.of unique vehicle IDs
ID=NaN(nveh,1); IDfreq=NaN(nveh,1);
MinT=NaN(nveh,1);MaxT=NaN(nveh,1);
MinY=NaN(nveh,1);MaxY=NaN(nveh,1);
```

```

THsum=NaN(nveh,1);
speed=NaN(nveh,1);
dist=NaN(nveh,1);TT=NaN(nveh,1);tvel=NaN(nveh,1);
THway=NaN(nveh,1);

i=1;j=1;freq=0;
tempID=dtmtrx(1,1);
tempMinT=dtmtrx(1,4); tempMaxT=dtmtrx(1,4);
tempMinY=dtmtrx(1,6); tempMaxY=dtmtrx(1,6);
Tsum=0;
while (i<=length(dtmtrx(:,1)))
    if dtmtrx(i,1)==tempID
        ID(j)=dtmtrx(i,1);IDfreq(j)=freq +1;
        THsum(j)=Tsum+dtmtrx(i,18); % to calculate sum of time headways
for a vehicle
    Tsum=THsum(j); % which will be used for the avg time
headway
    MinT(j)= nanmin(tempMinT,dtmtrx(i,4));
    MaxT(j)= nanmax(tempMaxT,dtmtrx(i,4));
    MinY(j)=nanmin(tempMinY,dtmtrx(i,6));
    MaxY(j)=nanmax(tempMaxY,dtmtrx(i,6));

else
    j=j+1;
    tempID= dtmtrx(i,1);
    tempMinT=dtmtrx(i,4);tempMaxT=dtmtrx(i,4);
    tempMinY=dtmtrx(i,6);tempMaxY=dtmtrx(i,6);
    freq=0;Tsum=0;
    ID(j)=dtmtrx(i,1);IDfreq(j)=freq+1;
    THsum(j)=Tsum+dtmtrx(i,18);Tsum=THsum(j);
    MinT(j)= nanmin(tempMinT,dtmtrx(i,4));
    MaxT(j)= nanmax(tempMaxT,dtmtrx(i,4));
    MinY(j)=nanmin(tempMinY,dtmtrx(i,6));
    MaxY(j)=nanmax(tempMaxY,dtmtrx(i,6));

end;
i=i+1;freq=freq+1;
end;

for i=1:nveh
    dist(i)=(MaxY(i)-MinY(i)); %feet
    TT(i)=(MaxT(i)-MinT(i))/1000; %seconds
    THway(i)=THsum(i)/IDfreq(i);
    %tvel(l)=dist(l)/TT(l);
end;

summ=[ID IDfreq dist TT THway tvel]; % MinT MaxT MinY MaxY];

outliers3=summ(:,2)<2; % reject vehicles with freq =1 or 0...ie.entered late
summ(any(outliers3,2),:)= []; %remove vehicle entered late

nv(k)=length(summ(:,1)); %number of vehicles in the delta_t time window
avgd(k)=mean(summ(:,3)); %average distance
sumtt(k)=sum(summ(:,4)); %sum of travel times for all the vehicles

```

```

avgtt(k)=mean(summ(:,4));%*****CHECK*****
tms(k)=mean(summ(:,6))/1.467;
%avgHa(k)=sum(summ(:,5))/nv(k); %Avg time headway (seconds)
avgHa(k)=mean(dtmtrx(:,18));
SMS(k)=(mean(summ(:,3))*nv(k)/sumtt(k)/1.467); % =
n*(d1+d2+d3...)/(tt1+tt2+tt3...) UNITS mph

flowh(k)=nearest(3600/avgHa(k));
%*****
%density for k will be the average of number of vehicles in that
%section for every milisecond
%length(find(A==3)) find frequency of 3 in vector A
dens=length(dtmtrx(:,4))/length(unique(dtmtrx(:,4)));% no of time-stamps
in k/no of unique time-stamps
density(k)=nearest(dens/(100/5280)/6); % in veh/mile/lane
flowd(k)=nearest(density(k)*SMS(k));
k=k+1;
Ts=Ts+delta_t;
summ=zeros(1,5);
outliers2=NaN(1,1);
else
    Ts=Ts+delta_t;
end;
end;
final=[nv avgd avgtt tms SMS density flowd flowh]; % summary

figure (1) %:<Speed-Flow plot>
plot(flowd,SMS,'ks',flowh,SMS,'+') ; %Speed flow plot
xlabel('Flow (vph)');ylabel('Speed(mph)');grid
off;legend('Flow=speed*density','Flow=1/headway');
figure (2)%<Flow-Density plot>
plot(density,flowd,'ks',density,flowh,'+') ; %flow-density plot
xlabel('Density(vplph)');ylabel('Flow(vph)');grid
off;legend('Flow=speed*density','Flow=1/headway');
figure (3)%<Speed-Density plot>
plot(density,SMS,'ks') ; %Speed-Density plot
xlabel('Density(vplph)');ylabel('Space Mean Speed(mph)');grid off;

```


APPENDIX A-2

```
% PROCEDURE . .STEP-1 RUN THIS FILE catas FIRST;
%                      STEP-2 Run gatool , with # of vars=2, m-file cat_max
%                      STEP-3 Run the file cat_check after substituting the t(1) and
t2;

FILE: catas
load c1; %file with AvgSp, AvgVol,AvgOc

Xcrt=42;%50 Xcrt=c1(1,4);42
Umax=15; %15 max volume
Vmax=21;%21 25 max. occupancy at max vol
t1=-12; % 0.58 4 angle of rotation can be negative
GF=(15/65);%15/65

len = length(c1);
avgX=c1(:,1);
avgU=c1(:,2);
avgV=c1(:,3);
X2=zeros(len,1);U2=zeros(len,1);V2=zeros(len,1);dumy=zeros(len,1);
for i=1:len
X2(i)=avgX(i)-Xcrt;
U2(i)=avgU(i)-Umax;
V2(i)=avgV(i)-Vmax;
end;

%to find the number of data points in congested area
lcg=0;
for i=1:len
    if (X2(i)<=0)
        lcg=lcg+1;
        dumy(i)=1;%dumy takes value 1 if the point is in congested region
    end;
end;
lucg =len-lcg;
Ucg=NaN(lcg,1); Vcg=NaN(lcg,1); %U2 and V2 values for congested region
Uug=NaN(lucg,1); Vug=NaN(lucg,1);

j=1;m=1;
for k=1:len
    if (X2(k)<=0)
        Ucg(j)=U2(k);
        Vcg(j)=V2(k);
        j=j+1;
    else
        Uug(m)=U2(k);
        Vug(m)=V2(k);
        m=m+1;
    end;
end;
end;
```

```

figure(1)
plot(Vcg,Ucg,'ks',Vug,Uug,'+') ; %U2 vs V2
xlabel('V2'); ylabel('U2'); grid on; legend('congested','uncongested');

V3cg=Vcg*GF;
V3ug=Vug*GF;

Ufc=zeros(lcg,1);Vfc=zeros(lcg,1);
for i=1:lcg
Ufc(i)=Ucg(i)*cosd(t1) -V3cg(i)* sind(t1);
Vfc(i)= Ucg(i)* sind(t1)+ V3cg(i)*cosd(t1);
end;
Ufu=zeros(lucg,1);Vfu=zeros(lucg,1);
for i=1:lucg
Ufu(i)=Uug(i)*cosd(t1) - V3ug(i)* sind(t1);
Vfu(i)= Uug(i)* sind(t1)+ V3ug(i)*cosd(t1);
end;

figure(2)
plot(Vfc,Ufc,'ks',Vfu,Ufu,'+') ; %U vs V or Uf vs Vf
xlabel('V'); ylabel('U'); grid on; legend('congested','uncongested');

Uf=zeros(len,1); Vf=NaN(len,1);
for i=1:len
Uf(i)=U2(i)*cosd(t1) - V2(i)*GF*sind(t1);
Vf(i)= U2(i)* sind(t1)+ V2(i)*GF*cosd(t1);
end;

Xf=X2;
crti =zeros(len,1);
crti(1,1)=Xcrt;
c2=[Xf Uf Vf crt]; % creates a variable (matrix) with the tranformed data
save('c2','c2'); % saves the matrix c2 with filename c2 in the directory

FILE: cat_max
function val_out=cat_max(t)

load c2; %file with X2,Uf,Vf
len=length(c2); Xf=c2(:,1); Uf=c2(:,2); Vf=c2(:,3);
%Xcrt=c2(1,4);% Check !!!23

nr=NaN(len,1);Xc=NaN(len,1);er=0;

for i=1:len
a=t(1)*Uf(i); b= t(2)*Vf(i);
p= [1 0 a b]; %Xf(i)^3+(t(1)*Uf(i)*Xf(i))+(t(2)*Vf(i));
r=roots(p);

if ((length(r)==3)&&isreal(r(1))&& isreal(r(2))&& isreal(r(3)))
nr(i)=3; % no. of roots
R=sort(r);
if (Vf(i)>0)

```

```

    Xc(i)=R(1);
else Xc(i)=R(3);
end;
else
nr(i)=1;
if (isreal(r(1)))
Xc(i)=r(1);
else
if (isreal(r(2)))
Xc(i)=r(2);
else
if (isreal(r(3)))
Xc(i)=r(3);
end;
end;
end;

er=er+(Xc(i)-Xf(i))^2;
end;

val_out=er;

FILE: cat_check
load c2; %file with X2,Uf,Vf

len=length(c2);
Xf=c2(:,1);
Uf=c2(:,2);
Vf=c2(:,3);
Xcrt=c2(1,4);% Check !!!23
t= [2.01655 -2.43677];%[];;
nr=NaN(len,1);Xc=NaN(len,1);
er=0;
nr=zeros(len,1);
xroots=NaN(len,3);
for i=1:len
a=t(1)*Uf(i); b= t(2)*Vf(i);
p= [1 0 a b]; %Xf(i)^3+(t(1)*Uf(i)*Xf(i))+(t(2)*Vf(i));
r=roots(p);
xroots(i,:)=r;
if (isreal(r(1))&& isreal(r(2))&& isreal(r(3)))
nr(i)=3; % no. of roots
R=sort(r);
if (Vf(i)>0)
Xc(i)=R(1)+Xcrt;
else Xc(i)=R(3)+Xcrt;
end;
else
nr(i)=1;
if (isreal(r(1)))
Xc(i)=r(1)+Xcrt;
else
if (isreal(r(2)))
Xc(i)=r(2)+Xcrt;

```

```

    else
        if (isreal(r(3)))
            Xc(i)=r(3)+Xcrt;
        end;
    end;
end;

er=er+(Xc(i)-Xf(i)-Xcrt)^2;
end;

Xac=Xf+Xcrt;
clf(figure(3));
figure(3)
plot(Xac,Xc,'+');
xlabel('Actual Speed (mph)'); ylabel('Predicted Speed (mph)'); grid on;

```

APPENDIX A-3

```
%start with the fitted model
%calculate the speed at near (<) capacity add a few vehicles recalculate
%the speed for increased flow
%find out the difference between congestion toll estimates of these two
%speed values
% repeat for different flow values 70, 80, 90, 100 % of capacity,
% how to address demand > capacity issue?

%empirical data- sudden speed decrease of 15 (or 20?) mph- notice the flow
%before that speed jump
clc;
clear all;
vo=54*1.609; qo=1684; vf=64*1.609;
alpha=0.39; %alpha<=1, beta>0
beta=(vo/vf)/(alpha-(vo/vf)*alpha);
beta2=vo/(vf-vo); kj=110;

oc=20;% operation cost+VTTS $/hr
flw=0;mat=[0 0 0 0 0 0 0 0 0 0]; %
while (flw<qo)

    Vhcm_l =round( fzero(@(V)Mhcm(V,flw,qo,vo,vf,alpha), [vo 0])/1.609);
    %modified HCM model
    Vhcm_u =round( fzero(@(V)Mhcm(V,flw,qo,vo,vf,alpha), [vo
    vf])/1.609);vhc=Vhcm_u*1.609;
    rhc=(oc/(vhc))*((vo-vhc*((alpha*beta)/(1+(alpha*beta))))/(alpha*(vhc-
    vo)));
    Vnf_l=(fzero(@(V2)Mnf(V2,flw,qo,vo,vf), [vo 0])/1.609); %Newell
    Franklin
    Vnf_u=(fzero(@(V2)Mnf(V2,flw,qo,vo,vf), [vo vf])/1.609);
    vnf=Vnf_u*1.609;ax=(1/beta2)*log((vf-vnf)/(vf-vo));bx=(vnf/vo)*((vf-
    vo)/(vf-vnf));
    rnf=1.609*(oc/(vnf))*((1-ax)/(bx-1+ax));
    Vva_l=round(fzero(@(V3)Mva(V3,flw,qo,vo,vf), [vo 0])/1.609); %Van
    Aerde Model
    Vva_u=round(fzero(@(V3)Mva(V3,flw,qo,vo,vf), [vo vf])/1.609);
    m=(2*vo-vf)/((vf-vo)^2);c2=1/(kj*(m+1/vf)); c1=m*c2; c3=(-c1+vo/qo-
    c2/(vf-vo))/vo;
    vva=Vva_u*1.609;a1x=c1+c2/(vf-vva)+c3*vva;b1x=c1-c2*vva/((vf-
    vva)^2)+c2/((vf-vva));
    rva=-(oc/vva)*(a1x/b1x)*1.609;
    % end;
    mat=[mat; flw, Vhcm_l, Vhcm_u, Vnf_l, Vnf_u, Vva_l,Vva_u rhc rnf rva];
    clear Vhcm_l Vhcm_u Vnf_l Vnf_u Vva_l Vva_u rhc rnf rva;
    flw=flw+1;
    clc;
end;

load D051606;%D051606;%Occ, Flow, SPeed%
dat=D051606;
len=length(dat); flow=dat(:,2); %veh/hr/ln
speed=dat(:,3)*1.609;%kmph
speedm=dat(:,3);
```

```

mat(1,:)=[]; %remove the first blank place holder row
flo=[(mat(:,1));(mat(:,1))]; %for adding the upper and lower speeds, flows
Vhc=[(mat(:,2));(mat(:,3))];Vnf=[(mat(:,4));(mat(:,5))];Vva=[(mat(:,6));(mat(:,7))];

rt=[0 200 400 500 700 1000 1200 1500 1684 1700 1800 1900 2000 2100 2200 2300
2400 2500 3000];
for i=1:length(rt)
    if (rt(1,i)<=qo)
        Vb(i,1)=vf/1.609; flb(i,1)=rt(1,i);
    else
        Vb(i,1)=((vf/1.609)*qo) / (qo+(vf/1.609)*(rt(1,i)-qo));flb(i,1)=rt(1,i);
    end;
end;

clear figure(1);
figure(1);plot(flow,speedm,'.',flo,Vhc,'v',flo,Vnf,'*',flo,Vva,'x',flb(:,1),Vb(:,1));
axis([0 2500 0 77]);
xlabel('flow in veh/h (Demand in veh/h for Bottleneck Model)');ylabel('Speed in mph');
grid on;
legend('Data','Modified HCM Model','Van Aerde Model','Newell-Franklin Model','Vickery Bottleneck Model');

clear figure(2); figure(2);
plot(mat(:,1),mat(:,8),'-.',mat(:,1),mat(:,9),'-.',mat(:,1),mat(:,10),'-.');
xlabel('flow in veh/h');ylabel('toll in $/mile');
legend('Modified HCM model','Newell-Franklin model','Van Aerde Model');

```